



EDAP+ TN on Quality Assessment of PlanetScope SuperDove

Author(s):



Digitally signed by Dr Samantha Lavender
DN: cn=Dr Samantha Lavender, o, ou,
email=sam.lavender@telespazio.com,
c=US
Date: 2024.04.18 16:47:05 +01'00'

Sam Lavender
Task 2 Team

Approval:

DocuSigned by:
Kevin Halsall
95EFDD4879A4CF...

Kevin Halsall
Task 2 Lead

Accepted:

Leonardo De
Laurentiis

Digitally signed by Leonardo De
Laurentiis
Date: 2024.04.18 11:40:26 +02'00'

Leonardo De Laurentiis
EDAP+ Technical Officer

EDAP+.REP.005

Issue: 1.0

18/04/24

AMENDMENT RECORD SHEET

The Amendment Record Sheet below records the history and issue status of this document.

| ISSUE | DATE | REASON |
|-------|----------|---|
| 0.1 | 13/09/23 | First Draft |
| 1.0 | 18/04/24 | Updated after feedback from ESA, and a revision of the MTF results and SNR plots to improve the analysis/reporting, and additional plot for the temporal geolocation. |
| | | |

TABLE OF CONTENTS

| | |
|---|-----------|
| 1. EXECUTIVE SUMMARY | 4 |
| 1.1 References | 4 |
| 1.2 Glossary | 6 |
| 1.3 Cal/Val Maturity Matrices | 7 |
| 1.3.1 Summary Cal/Val Maturity Matrix | 7 |
| 1.3.2 Validation Cal/Val Maturity Matrix | 8 |
| 2. DATA PROVIDER DOCUMENTATION REVIEW | 10 |
| 2.1 Product Information | 10 |
| 2.2 Metrology | 15 |
| 2.3 Product Generation | 17 |
| 3. DETAILED VALIDATION – RADIOMETRY | 19 |
| 3.1 Introduction | 19 |
| 3.2 Data | 19 |
| 3.3 Absolute Radiometric Calibration Accuracy (RadCalNet) | 20 |
| 3.3.1 Method | 20 |
| 3.3.2 Results | 20 |
| 3.4 Temporal Radiometric Calibration Accuracy (Stability) | 23 |
| 3.4.1 Method - PICS | 23 |
| 3.4.2 Results – PICS | 23 |
| 3.4.3 Method – RadCalNet | 24 |
| 3.4.4 Results – RadCalNet | 24 |
| 3.5 Results Compliance | 26 |
| 4. DETAILED VALIDATION – GEOMETRIC | 27 |
| 4.1 Introduction | 27 |
| 4.2 Data | 27 |
| 4.3 Absolute Geolocation Accuracy | 27 |
| 4.3.1 Method | 27 |
| 4.3.2 Results | 27 |
| 4.4 Temporal Geolocation Accuracy | 28 |
| 4.4.1 Method | 28 |
| 4.4.2 Results | 29 |
| 4.5 Inter-band Registration Accuracy | 31 |
| 4.5.1 Methods | 31 |
| 4.5.2 Results | 31 |
| 4.6 Results Compliance | 32 |
| 5. DETAILED VALIDATION – IMAGE QUALITY | 36 |



| | | |
|-------------------|--|-----------|
| 5.1 | Visual inspections | 36 |
| 5.1.1 | Method | 36 |
| 5.1.2 | Results | 36 |
| 5.1.2.1 | Usable Data Mask | 36 |
| 5.1.2.1.1 | Information | 36 |
| 5.1.2.1.2 | Assessment | 38 |
| 5.1.2.2 | Other visual inspection findings | 39 |
| 5.1.2.3 | Metadata information via QGIS | 40 |
| 5.2 | Signal-To-Noise Ratio (SNR) | 42 |
| 5.2.1 | Method | 42 |
| 5.2.2 | Results | 43 |
| 5.3 | Modulation Transfer Function (MTF) | 45 |
| 5.3.1 | Data | 45 |
| 5.3.2 | Method | 45 |
| 5.3.3 | Results | 47 |
| 5.4 | Results Compliance | 48 |
| APPENDIX A | Products analysed from the Mission Test Dataset | 50 |

1. EXECUTIVE SUMMARY

This technical note details the results of the mission data quality assessments (including geometric calibration, radiometric calibration, and image quality) performed on a sample of products generated for SuperDove imagery from a constellation of commercial Earth Observation (EO) optical satellites operated by Planet.

The aforementioned mission data quality assessments are performed in accordance with the assessment guidelines (as detailed in [RD-1], [RD-2] and [RD-3]) that constitute the European Space Agency (ESA) Earthnet Data Assessment Project's (EDAP) *Best Practice Guidelines* and *EO Mission Data Quality Assessment Framework*. An important representation of the latter framework, constructed by the National Physical Laboratory (NPL), is what is known as *the summary maturity matrix* and the detailed *validation maturity matrix*. It is a diagrammatic summary of the following:

- **Documentation Review:** the EDAP Optical team reviews materials (e.g. data and documentation) provided by the data provider or operator, some of which may not be publicly available, or the scientific community (e.g. published papers). The results are detailed in Section 2 (covering the first four columns of the summary maturity matrix).
- **Detailed Validation:** the EDAP Optical team performs data quality assessments (i.e. validation assessments), independently of any validation assessments performed by the data provider and / or operator. These validation results, summarised in the summary maturity matrix and the validation maturity matrix, are detailed in Sections 3 - 5).

The above assessments are performed by the EDAP Optical team using the appropriate in-house and open-source ad-hoc scripts / tools [RD-4].

It is important to note that the purpose of the aforementioned framework is to ensure that delivered satellite mission EO data is fit for purpose, and all decisions regarding the inclusion of a mission as an ESA Third Party Mission can be made fairly and with confidence.

1.1 References

The following is a list of reference documents with a direct bearing on the content of this proposal. Where referenced in the text, these are identified as [RD-n], where 'n' is the number in the list below:

- RD-1. EDAP Best Practice Guidelines, EDAP.REP.001, v1.2, September 2019.
- RD-2. EDAP.REP.001 Earth Observation Mission Quality Assessment Framework, Issue 2.2, December 2022.
- RD-3. EDAP.REP.002 Earth Observation Mission Quality Assessment Framework – Optical Guidelines, Issue 2.1, October 2021.
- RD-4. EDAP+ TN on Methods and Reference Data for Optical Data quality Assessments, EDAP+.REP.004, v1.1, July 2023.
- RD-5. Françoise Viallefont-Robinet, Dennis Helder, Renaud Fraisse, Amy Newbury, Frans van den Bergh, Donghan Lee, Sébastien Saunier.. Comparison of MTF measurements using edge method: towards reference data set. Optics Express, Optical Society of America, 2018, 26 (26), pp.33625-33648. (hal-02055611)

- RD-6. KARIOS Image Matching Tool: Software User Manual, EDAP+ SUM 01, Version 1, June 2023.
- RD-7. Planet Imagery Product Specifications, dated May 2022: https://assets.planet.com/docs/Planet_Combined_Imagery_Product_Specs_letter_sc_reen.pdf
- RD-8. EDAP Technical Note on Quality Assessment for SuperDove, EDAP.REP.041, Issue: 1.0, January 2022
- RD-9. PlanetScope: <https://developers.planet.com/docs/data/planetscope/>
- RD-10. STAC Index: <https://stacindex.org/>
- RD-11. OGC GML 3.1.1 Application Schema for Earth Observation Products Version 0.9.1 (2007): https://portal.ogc.org/files/?artifact_id=22161
- RD-12. On-orbit Radiometric Calibration of the Planet Satellite Fleet: https://assets.planet.com/docs/radiometric_calibration_white_paper.pdf
- RD-13. Planet L1 Data Quality Reports: <https://support.planet.com/hc/en-us/articles/360037649554-L1-Data-Quality-Reports-for-the-PlanetScope-Constellation#>
- RD-14. JACIE Presentation on PlanetScope (2016): <https://calval.cr.usgs.gov/apps/sites/default/files/jacie/JACIE-Presentation-Pre-launch-Calibration-of-the-Planet-Labs-PlanetScope-Constellation-1.pdf>
- RD-15. JCGM, "Evaluation of measurement data - Guide to the expression of uncertainty in measurement," 100, 2008: https://www.bipm.org/utis/common/documents/jcgm/JCGM_100_2008_E.pdf
- RD-16. The Spectral Response of Planet Doves: Pre-launch Method and Results, C. Pritchett et al., CALCON 2020: <https://digitalcommons.usu.edu/cgi/viewcontent.cgi?article=1399&context=calcon>
- RD-17. Bouvet, M.; Thome, K.; Berthelot, B.; Bialek, A.; Czapla-Myers, J.; Fox, N.P.; Goryl, P.; Henry, P.; Ma, L.; Marcq, S.; Meygret, A.; Wenny, B.N.; Woolliams, E.R. RadCalNet: A Radiometric Calibration Network for Earth Observing Imagers Operating in the Visible to Shortwave Infrared Spectral Range. Remote Sens. 2019, 11, 2401, <https://doi.org/10.3390/rs11202401>
- RD-18. RadCalNet Quickstart Guide: https://www.radcalnet.org/resources/RadCalNetQuickstartGuide_20180702.pdf
- RD-19. Zanoni, "IKONOS Signal-to-Noise Ratio Estimation", March 25-27, 2002, JACIE Workshop, 2002 <https://ntrs.nasa.gov/search.jsp?R=20040004380>
- RD-20. EDAP Technical Note on Methods and Reference Data for Optical Data Quality Assessments, EDAP+.REP.004, Issue: v1.0. Available online at: https://earth.esa.int/eogateway/documents/d/earth-online/edap-rep-004_1-0-edap-tn-on-methods-and-reference-data-for-optical-data-quality-assessments-v1-0

RD-21. QGIS MTF Estimator Plugin: https://github.com/JorgeGIIIG/MTF_Estimator

1.2 Glossary

The following acronyms and abbreviations have been used in this Report.

| | |
|------|--|
| BOA | <i>Bottom of Atmosphere</i> |
| BRDF | Bidirectional Reflectance Distribution Function |
| CEOS | <i>Committee on Earth Observation Satellites</i> |
| DN | Digital Number |
| EDAP | Earthnet Data Assessment Pilot |
| EO | Earth Observation |
| ESA | European Space Agency |
| GUM | <i>Guide to the Expression of Uncertainty in Measurement</i> |
| IVOS | InfraRed and Visible Optical Sensors |
| MTF | Modulation Transfer Function |
| NIR | Near InfraRed |
| NPL | National Physical Laboratory |
| PICS | Pseudo Invariant Calibration Site |
| RMSE | <i>Root Mean Square Error</i> |
| ROI | Region of Interest |
| SNR | Signal to Noise Ratio |
| STAC | Spatial Temporal Asset Catalog |
| TOA | <i>Top of Atmosphere</i> |
| UDM2 | Usable Data Mask |
| WGCV | Working Group for Calibration and Validation |

1.3 Cal/Val Maturity Matrices

1.3.1 Summary Cal/Val Maturity Matrix

| Data Provider Documentation Review | | | Validation Summary | Key |
|------------------------------------|--|-----------------------------|---|----------------|
| Product Information | Metrology | Product Generation | | |
| Product Details | Sensor Calibration & Characterisation | Calibration Algorithm | Measurement Validation Method | Not Assessed |
| Availability & Accessibility | Geometric Calibration & Characterisation | Geometric Processing | Measurement Validation Results Compliance | Not Assessable |
| Product Format, Flags & Metadata | Metrological Traceability Documentation | Retrieval Algorithm | Geometric Validation Method | Basic |
| User Documentation | Uncertainty Characterisation | Mission-Specific Processing | Geometric Validation Results Compliance | Good |
| | Ancillary Data | | | Excellent |
| | | | | Ideal |
| | | | | Not Public |

Figure 1-1: Summary Cal/Val Maturity Matrix

1.3.2 Validation Cal/Val Maturity Matrix

The Optical Validation Cal/Val Maturity Matrix [RD-3] is instrument-domain specific and provides a more complete report of the assessments behind the Validation Summary – breaking down the validation into the methodologies used and the results obtained.

A summary of the EDAP validation results is shown in Table 1-1, concerning the geometric assessment and sensor spatial resolution. Regarding the operator claims, a grade of 'Excellent' is assigned for absolute accuracy and inter-band registration, while the MTF results were not considered sufficient for grading, and Planet did not assess the temporal stability.


| Geometric Validation | | | Key Not Assessed Not Assessable Basic Good Excellent Ideal  Not Public |
|----------------------------------|---|---|---|
| | Method | Results Compliance | |
| Sensor Spatial Resolution (MTF) | Knife Edge [RD-5] approach would be classed higher, but an MTF target is not used, so the methodology is less certain | Insufficient results obtained for the methodology applied | |
| Absolute Geolocation Accuracy | KARIOS Tool [RD-6] and Raster Reference | Less than 10.0 m RMSE | |
| Inter-band Registration Accuracy | KARIOS Tool | Less than a pixel achieved | |
| Temporal Geolocation Accuracy | KARIOS Tool applied to the Analysis Ready products | Not assessed by Planet as a time-series comparison, results do show less than a pixel stability | |

Figure 1-2: Geometric Validation Cal/Val Maturity Matrix

Table 1-1: Geometric Validation Results

| | Inter-band Accuracy [m] | Absolute Geolocation Accuracy [m] | Temporal Geolocation Accuracy [m] |
|----------------------|---|---|--|
| EDAP+, see Section 4 | Green-Blue: 4.31 RMSE (Mean) / 6.62 CE90 Green - Red: 4.18 RMSE (Mean) / 6.31 CE90 Green - NIR: | 4.08 RMSE (Mean) / 5.56 CE90 [based on seven products] | Shown in Section 4.4 [calculated for the trial Analysis Ready products] |

| | | | |
|---|---|---|--|
| | 6.41 RMSE (Mean) / 9.91 CE90 [based on nine products] | | |
| Planet [RD-13] | Green-Blue 0.32 RMSE (90th percentile, PCTL90) Green-Red 0.3 RMSE (PCTL90) Green-NIR: 0.98 RMSE (PCTL90) [Sample Size: 10845] | 5.75 RMSE (PCTL90) / 6.21 CE90 [Sample Size: 8806] | <i>Analysis not undertaken in the same way</i> |
| Results reported in the previous EDAP assessment [RD-8] | Green-Blue 2.9 RMSE / 4.9 CE90 Green-Red 2.5 RMSE / 3.7 CE90 Green-NIR: <i>Not assessed</i> [from one product] | 8.9 RMSE / 13.7 CE90 [from one product] | <i>Not undertaken</i> |

Regarding radiometric calibration, including Signal to Noise Ratio (**SNR**), a summary of EDAP validation results is listed in Table 1-2. An EDAP grade of 'Excellent' is reached for the RadCalNet absolute radiometric assessment and SNR. The temporal stability is not assessed.

Table 1-2: Radiometric Validation Results

| Radiometric Validation | | | Key |
|------------------------|--|---|--------------|
| | Method | Results Compliance | |
| Absolute Calibration | RadCalNet based method | <10% (achieved), but in comparison to the Planet RadCal matchup results reported the number of products used was small | Excellent |
| Signal to Noise | [RD-19] Statistics | 50 - 100 for all bands over both sites (La Crau and Libya-4), with values higher than reported by Planet | Good |
| Temporal Stability | Pseudo Invariant Calibration Site (PICS) with Sentinel-2 as the reference | Reported results in the Q1 2023 Quality Report [RD-13] are the same differences as the RadCalNet values. Data not suitable for a PICS analysis, but we found a good agreement with the RadCalNet surface measurements at La Crau. | Not Assessed |

Figure 1-3: Radiometric Validation Cal/Val Maturity Matrix

2. DATA PROVIDER DOCUMENTATION REVIEW

2.1 Product Information

SuperDove were built with the PSB telescope and the same filter response as PS2.SD (Dove-R) instrument [RD-9]. The instruments capture Red, Green, Blue, and Near InfraRed (NIR) bands, as well as a new Red Edge, Green I, Coastal Blue, and Yellow bands that have not been supplied. The Scene products are approximately 32.5 x 19.6 sq km, and the earliest imagery was acquired mid-March 2020, and the PlanetScope constellation provides images at approximately 3 m per pixel resolution.

The primary data used in this technical note is the Level 3 (L3) PlanetScope Ortho Scene Product is orthorectified, and a scaled Top of Atmosphere Radiance (at sensor) or Surface Reflectance image product [RD-7]. The Product Details shown in the table below are contained within the supplied products' metadata. It is fully understood that some of the requested information is available from the Planet website.

Each **product** for assessment was supplied as follows:

1. Folder, e.g. **20210314_094331_43_2423_DOV_MS_L3A**, containing:
 - a. manifest.json
 - b. 20210314_094331_43_2423_metadata.json
 - c. Folder: **analytic_udm2**, containing:
 - i. 20210314_094331_43_2423_3B_AnalyticMS.tif
 - ii. 20210314_094331_43_2423_3B_AnalyticMS_metadata.xml
 - iii. 20210314_094331_43_2423_3B_udm2.tif

The details shown below can be found within file (ii) underlined above.

For the temporal geolocation assessment (Section 4.4) we used the supplied Analysis Ready PlanetScope Backfill data that was supplied on a trial basis. Planet Fusion Backfill data and the Analysis Ready data were also supplied and used in the radiometric stability analysis (Section 3.4).

For these two time-series products, the data was provided via an Amazon Web Service S3 bucket with the different components of each product being in its own folder. The data was in a directory structure, with a time-series of over 3000 products available between 01 January 2018 and 23 July 2023. This methodology for supplying data reflects the move to cloud-native formats, with the Spatial Temporal Asset Catalog (STAC) [RD-10] JSON files providing the metadata. As the data was on trial, there was no user documentation, so information was missing in terms of the details of the processing, and Planet assessed quality information.

| Product Details | |
|-----------------|---|
| Good | |
| Justification | <i>The details below in this table are for the L3 product on the left, and the trial time-series products (Analysis Ready and Fusion) on the right. As can be seen from the comparison, the time-series products have a subset of the L3 product information. There was an issue with the trial time-series products supplied as the STAC files were the same for the Analysis Ready and Fusion products – containing metadata referencing the Fusion products.</i> |

| Product Details | | |
|-----------------------------|--|--|
| Product Name | <eop:fileName>20210314_094331_43_2423_3B_AnalyticMS.tif</eop:fileName> | Just the date, e.g. 2021-03-14.tif |
| Sensor Name | <eop:shortName>PSB.SD</eop:shortName> | "planetscope" |
| Sensor Type | <eop:sensorType>OPTICAL</eop:sensorType> | Not shown |
| Mission Type | Not shown | "platform": "planet" |
| Mission Orbit | <eop:orbitType>LEO-SSO</eop:orbitType> | Not shown |
| Product Version Number | <eop:processorVersion>4.1.4</eop:processorVersion> | "pipeline_version": "0.1.2" |
| Product ID | <eop:identifier>20210314_094331_43_2423_3B_AnalyticMS</eop:identifier> | "id": "31N/27E-201N/2021-03-14" |
| Processing level of product | <eop:productType>L3B</eop:productType> | Not shown |
| Measured Quantity Name | Indirectly given as Digital Number (DN) by the following text: <ps:bandNumber>1</ps:bandNumber> <!-- Multiply by radiometricScaleFactor to convert DNs to TOA Radiance (watts per steradian per square metre --> <ps:radiometricScaleFactor>0.01</ps:radiometricScaleFactor> <!-- Multiply by reflectanceCoefficient to convert DNs to TOA Reflectance --> <ps:reflectanceCoefficient>2.655732307428764e-05</ps:reflectanceCoefficient> | "title": "Surface Reflectance" "scale": 0.0001 "offset": 0 |
| Measured Quantity Units | Yes (see item above) | Not shown |
| Stated Measurement Quality | Not shown | Not shown |
| Spatial Resolution | <eop:resolution uom="m">3.0000</eop:resolution> | "spatial_resolution": 3 |
| Spatial Coverage | <gml:coordinates>5.53220275375975,43.3046080378877 5.96924024596795,43.2288551663393 5.90754876310128,43.0382279237451 5.47090173508466,43.1145828773346 5.53220275375975,43.3046080378877</gml:coordinates> | "geometry": {"type": "Polygon", "coordinates": [[[4.832304693393312, 43.5542750952779], [5.12924730001119, 43.54912862178922], [5.136895125033481, 43.765075859380445], [4.83888754209512, 43.77026105765286], [4.832304693393312, 43.5542750952779]]]}, "bbox": |

| Product Details | | |
|-------------------------------|---|---|
| | | [4.832304693393312, 43.54912862178922, 5.136895125033481, 43.77026105765286] |
| Temporal Resolution | Not shown | Not shown |
| Temporal Coverage | Although the following is stated, ideally more accuracy would be required to differentiate start/stop times: <code><gml:TimePeriod> <gml:beginPosition>2021-03-14T09:43:31+00:00</gml:beginPosition> <gml:endPosition>2021-03-14T09:43:31+00:00</gml:endPosition></code> | "datetime": "2021-03-14" |
| Point of Contact | Indirectly given, since Schemas within the metadata point the user to the Planet website, e.g. <code>xmlns:ps="http://schemas.planet.com/p/s/v1/planet_product_metadata_geocorrected_level"</code> | Not shown |
| Product locator (DOI/URL) | Not shown | Not shown |
| Conditions for access and use | <code><ps:licenseType>20160101 - Inc - Single User</ps:licenseType> <ps:resourceLink xlink:title="PL EULA" xlink:href="https://assets.planet.com/docs/20160101_Inc_SingleUser.txt"/></code> | Not shown |
| Limitations on public access | Yes (see item above) | Not shown |
| Product Abstract | Not shown | Not shown |

| Availability & Accessibility | |
|--------------------------------|--|
| Grade: Good | |
| Justification | <p><i>Planet is a commercial satellite operator; low-resolution images can be viewed from their website before purchase.</i></p> <p><i>The commercial Planet products would not be expected to conform to research-level access principles.</i></p> <p><i>However, accessibility is Good, and availability is Excellent.</i></p> |
| Compliant with FAIR principles | <p>https://www.go-fair.org/fair-principles/</p> <p>No. For example, one item that we believe is not achieved: "A2. Metadata are accessible, even when the data are no longer available"</p> |

| Availability & Accessibility | |
|------------------------------|------------------------|
| Data Management Plan | Not seen. |
| Availability Status | Commercially available |

| Product Format | |
|----------------------|---|
| Good | |
| Justification | <i>The data exist in a documented standard file format, but it isn't clear that standard naming conventions are used. There are documented metadata and data flags.</i> |
| Product File Format | <p>The L3 GeoTIFF file with associated mask (udm2) tif file and metadata xml file, e.g. 20210314_094331_43_2423_3B_AnalyticMS.tif 20210314_094331_43_2423_3B_udm2.tif 20210314_094331_43_2423_3B_AnalyticMS_metadata.xml</p> <p>For the time-series products, the data was provided via an Amazon Web Service S3 bucket, with the different components of each product being in its own folder.</p> <p>UTM-24000/31N/[27E-200N or 27E-201N for the two supplied tiles]/</p> <p>ARP-QA/ - Analysis Ready Product, QA GeoTIFF ARP-SR/ - Analysis Ready Product, Surface Reflectance GeoTIFF ARP-STAC/ - Analysis Ready Product, STAC JSON PF-QA/ - Planet Fusion Product, QA GeoTIFF PF-SR/ - Planet Fusion Product, Surface Reflectance GeoTIFF PF-STAC/ - Planet Fusion Product, STAC JSON</p> |
| Metadata Conventions | The XML files associated with the L3 GeoTIFFs are compliant with the OGC GML 3.1.1 Application Schema for Earth Observation Products Version 0.9.1 (2007-08-01) [RD-11], and the time-series products are generated using STAC [RD-10] version 1.0.0 |
| Analysis Ready Data? | The ARD products are separate to the L3 GeoTIFFs |

| User Documentation | | |
|-------------------------|---|---|
| Grade: Good | | |
| Justification | <p>The Planet website https://www.planet.com/ has many pages of information that are useful and easily available for the regular user of the products, some of which are itemised below.</p> <p>Due to the commercial nature of the products, detailed technical documentation may not always be freely available for view, but recently details of the radiometric calibration have been made available.</p> | |
| Document | Reference | QA4ECV Compliant |
| Product User Guide | Understanding PlanetScope Instruments https://developers.planet.com/docs/apis/data/sensors/ | http://www.qa4ecv.eu/ There is no overarching user guide, and instead several sources produce the user needed information. |
| PlanetScope Overview | https://developers.planet.com/docs/data/planet-scope/ | |
| Product Specifications | Planet Imagery Product Specifications, dated May 2022 [RD-7] | |
| Calibration information | <ul style="list-style-type: none"> On-orbit Radiometric Calibration of the Planet Satellite Fleet [RD-12] Planet L1 Data Quality Reports for PlanetScope [RD-13] | |
| ATBD | Not available | No |

2.2 Metrology

| Sensor Calibration & Characterisation | |
|---------------------------------------|---|
| Good | |
| Justification | <p>Conference documents (public) are available detailing pre-flight calibration, demonstrating that pre-flight activities have been performed. However, this material is not of sufficient detail to assess the pre-flight calibration approach.</p> <p>Post-launch calibration and characterisation activities are regularly performed, and the method is described in dedicated L1 Quality Reports that are publically available. In addition, Planet is using appropriate community infrastructure (Committee on Earth Observation Satellites (CEOS), PICS, RadCalNet) to perform analyses.</p> |
| References | <ul style="list-style-type: none"> Planet L1 Data Quality Reports for PlanetScope [RD-13] Joint Agency Commercial Imagery Evaluation (JACIE) presentation on PlanetScope (2016) [RD-14] |

| Geometric Calibration & Characterisation | |
|--|--|
| Good | |
| Justification | <p>There is a basic description of the geometric calibration processing in the Product specification [RD-7] alongside the resulting characterisation regarding Root Mean Square Error (RMSE). A more detailed description is present in the quarterly L1 Quality Reports, including further measures for characterisation such as CE90 (Circular Error probable at 90th percentile). It would be helpful if users were pointed to these Quality Reports from inside the Product Specification.</p> |
| References | <ul style="list-style-type: none"> Planet Imagery Product Specifications, dated May 2022 [RD-7] Planet L1 Data Quality Reports for PlanetScope [RD-13] |

| Metrological Traceability Documentation | |
|---|--|
| Not Assessable | |
| Justification | <p>No traceability chain is known to be documented.</p> <p>There is room for improvement concerning the product metadata, for which information on measurement quality and traceability of ancillary data is missing.</p> <p>Regarding quality data, the JSON files accompanying the L3 orthorectified products contain whole scene parameters (such as percentages for clouds, haze, shadow, and snow) alongside a quality_category that is standard or test. These are missing from the JSON files accompanying the Analysis</p> |

| | |
|------------|--|
| | <p>Ready/Fusion products. For these time-series products, the JSON files indicate there is metadata for pixel provenance and the number of FORCE L8 / L9 / S2 reference scenes used during calibration, but the expected accompanying values are missing. Also, the same JSON files were present for both the Analysis Ready and Fusion products, so it appears that the Fusion JSON files were supplied for the Analysis Ready Products.</p> <p>To obtain a higher assessment grade, a per-product error/uncertainty would be required alongside the ancillary data used.</p> |
| References | <ul style="list-style-type: none"> Planet L1 Data Quality Reports for PlanetScope [RD-13] |

| Uncertainty Characterisation | |
|------------------------------|---|
| Good | |
| Justification | <p>The Quarterly Reports show a comprehensive analysis of the most common product performance quality items based on representative datasets and comparisons with other sensors. However, it is not clear if the Guide to the Expression of Uncertainty in Measurement (GUM) has been applied.</p> |
| References | <ul style="list-style-type: none"> Planet L1 Data Quality Reports for PlanetScope [RD-13] Guide to the Expression of Uncertainty in Measurement [RD-15] |

| Ancillary Data | |
|----------------|---|
| Basic | |
| Justification | <p>Ancillary data/information is available via the metadata, e.g. for the L3 products the viewing and illumination angles but not the sensor altitude. The relative spectral response is available via presentations [RD-16] and web documentation. Additional information, such as the used Digital Elevation Model, is reported in the Quality Reports but not given in the metadata.</p> |
| References | <ul style="list-style-type: none"> Planet L1 Data Quality Reports for PlanetScope [RD-13] The Spectral Response of Planet Doves: Pre-launch Method and Results [RD-16] |

2.3 Product Generation

| Calibration Algorithm | |
|-----------------------|--|
| Good | |
| Justification | <i>The Product Specification and L1 Quality Reports document the radiometric calibration approach. The calibration applied is considered “fit for purpose” regarding the mission’s stated performance for all expected use cases. However, the full details are not available i.e., the level of an ATBD as used for space agency missions. This is not unexpected for a commercial company.</i> |
| References | <ul style="list-style-type: none"> Planet Imagery Product Specifications [RD-7] Planet L1 Data Quality Reports for PlanetScope [RD-13] |

| Geometric Processing | |
|----------------------|--|
| Good | |
| Justification | <i>The geometric processing is partially documented in Product Specification and L1 Quality Reports, particularly information regarding sensor modelling and ortho-processing. However, information to fully understand product geometry is not available i.e., the level of an ATBD as used for space agency missions. This is not unexpected for a commercial company.</i> |
| References | <ul style="list-style-type: none"> Planet Imagery Product Specifications [RD-7] Planet L1 Data Quality Reports for PlanetScope [RD-13] |

| Retrieval Algorithm | |
|---------------------|---|
| Basic | |
| Justification | <i>Planet can deliver surface reflectance products derived from the standard Planet Analytic (Radiance) Product that is processed to Top of Atmosphere (TOA) reflectance and then atmospherically corrected to Bottom of Atmosphere (BOA) or surface reflectance. As discussed in the Product Specification, Planet uses the 6S radiative transfer model with ancillary data from MODIS to account for atmospheric effects on the observed signal at the sensor. However, the full details are not available i.e., the level of an ATBD as used for space agency missions. This is not unexpected for a commercial company.</i> |
| References | <ul style="list-style-type: none"> Planet Imagery Product Specifications [RD-7] |

| Mission-Specific Processing | |
|-----------------------------|---|
| Not Assessed | |
| Additional Processing | |
| Justification | <i>The time-series product processing has been addressed under the previous box, 'Retrieval Algorithm'.</i> |
| Reference | - |

3. DETAILED VALIDATION – RADIOMETRY

3.1 Introduction

The radiometry analysis is based on a comparison to in-situ measurements or other satellites, such as Sentinel-2, which are considered radiometrically stable and highly characterised. For the work undertaken, described in detail within this Section, the overall approach to the radiometric validation is graded as 'Good' as several of the approaches are mature, but the temporal analysis is less mature.

3.2 Data

Data over La Crau, Gobabeb, and Libya-4 were assessed for radiometric accuracy and are listed in Table 3-1 to Table 3-3, respectively.

Table 3-1. La Crau data used to assess the absolute radiometric accuracy.

| Constellation | Dates | Satellites |
|---------------|------------------------|------------|
| Flock-4V | 29/07/2021 | 2426 |
| | 30/03/2021 | 2403 |
| | 06/04/2021 | 2403 |
| Flock-4S | 20/11/2021 | 2423 |
| | 06/09/2021 | 2423 |
| | 18/10/2021 | 2423 |
| Flock-4EP | 25/10/2021 | 2251 |
| | 25/05/2021 | 2251 |
| | 09:47:58 | 2251 |
| | 25/05/2021 09:48:01 | |

Table 3-2. Gobabeb data used to assess the absolute radiometric accuracy.

| Constellation | Dates | Satellites |
|---------------|------------|------------|
| Flock-4V | 27/06/2021 | 2426 |
| | 02/03/2021 | 2426 |
| | 15/12/2021 | 2426 |
| Flock-4EP | 03/06/2021 | 2264 |
| | 03/06/2021 | 2264 |
| | 25/04/2021 | 2251 |

Table 3-3. Libya-4 data used to assess the absolute radiometric accuracy.

| Constellation | Dates | Satellites |
|---------------|------------|------------|
| Flock-4V | 03/01/2021 | 2403 |
| | 03/04/2021 | 2426 |
| | 01/01/2021 | 2426 |

| | | |
|-----------|--|----------------------|
| Flock-4S | 20/12/2021 08:14:35 20/12/2021 08:14:31 | 2449 2449 |
| Flock-4EP | 29/01/2021 13/03/2021 23/01/2021 | 2251 2251 2251 |

3.3 Absolute Radiometric Calibration Accuracy (RadCalNet)

3.3.1 Method

The method used to determine the absolute radiometric calibration accuracy of the sensor's bands is based on comparing the top-of-atmosphere reflectance values derived from the sensors acquisitions of the chosen RadCalNet [RD-17] calibration sites with the simulated top-of-atmosphere reflectance values.

The RadCalNet calibration sites, operated by the CEOS Working Group for Calibration and Validation (**WGCV**) InfraRed and Visible Optical Sensors (**IVOS**), provides the scientific community with the following:

- Simulated Top-of-Atmosphere reflectance values (MODTRAN), derived from both in-situ surface and atmosphere measurements (e.g., surface pressure, columnar water vapour, columnar ozone, aerosol optical depth, etc.) that are SI-traceable, at:
- 30-minute intervals between 09:00 and 15:00 local standard time (cloud-free data only), and 10 nm spectral sample intervals between 400 nm and 1000 nm.

As mentioned in the Quick Guide [RD-18], the RadCalNet simulated top-of-atmosphere reflectance spectra are representative nadir view observations only. Comparison to space sensor reflectance measurements should be exercised with caution when the sensor viewing zenith angle deviates significantly from the nadir as both atmospheric and surface non-Lambertian behaviour can lead to significant deviation from at nadir simulated signal. However, the acquisition incidence angle of all supplied SuperDove products was less than 10°, so Bidirectional Reflectance Distribution Function (**BRDF**) normalisation has not been performed.

Finally, the percentage difference between sensor top-of-atmosphere reflectances (ρ_b work) and simulated sensor top-of-atmosphere reflectances (ρ_b simulated), using RadCalNet data, is calculated as follows:

$$\rho_b = ((\rho_b \text{ simulated} - \rho_b \text{ work}) / (\rho_b \text{ simulated})) * 100$$

A simple ratio, $\rho_b \text{ simulated} / \rho_b \text{ work}$ is also reported.

3.3.2 Results

From Figure 3-1, it can be seen that the La Crau site is in the middle of an open area where there is limited spatial variation, although there are some spatial features further away than

the SuperDove kernel being used – the site is flat but is intersected by field boundaries that include roads and buildings.

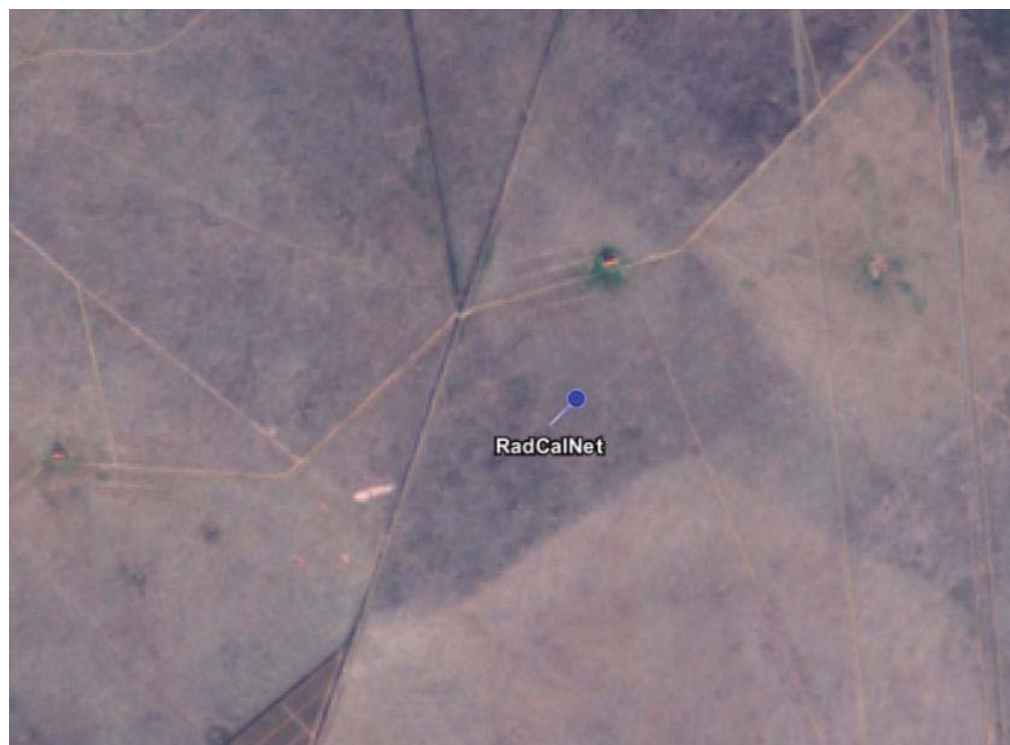


Figure 3-1: La Crau location on Sentinel-2 Level 1 image (18 March 2020), with the RadCalNet site location as a pin marker.

The calibration results based on in-situ RadCalNet data are described by showing the steps involved, implemented within a series of Jupyter notebooks. Figure 3-2 shows an example plot of the TOA RadCalNet reflectance spectra for La Crau (LCFR) and all the date/time matching RadCalNet spectra convolved to the SuperDove bands.

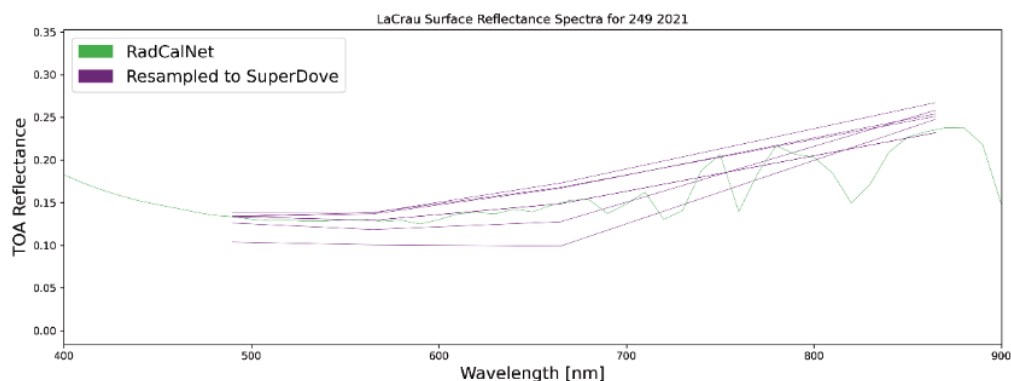


Figure 3-2: Convolution of the RadCalNet reflectance spectra into the SuperDove bands for La Crau.

For each date in the RadCalNet series, an input SuperDove file is looked for, and the data extracted for the time of satellite acquisition with the two spectra compared (Figure 3-3).

The actual SuperDove data is plotted as the mean of the kernel, with the vertical bars showing the standard deviation.

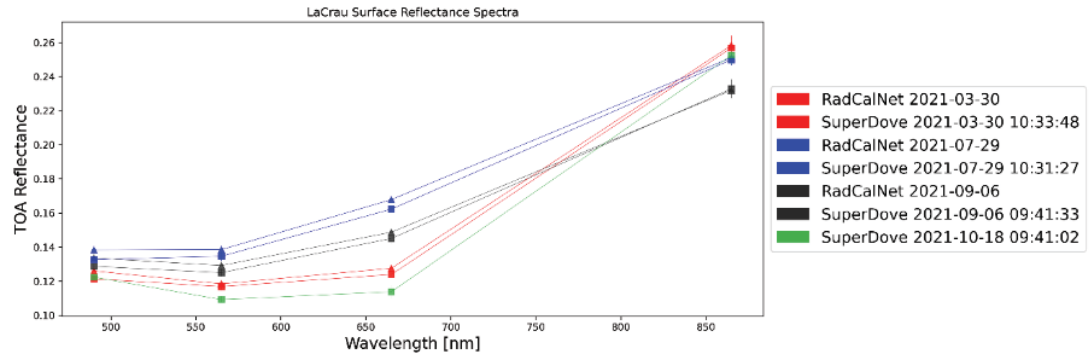


Figure 3-3: Comparison of SuperDove data to RadCalNet convolved to the SuperDove bands for the La Crau site.

Figure 3-4 shows the calculated percentage difference between the SuperDove and convolved RadCalNet data. All bands have higher values than the RadCalNet data except for the NIR band that has two values closer to zero, with one product (06/09/2021) being lower.

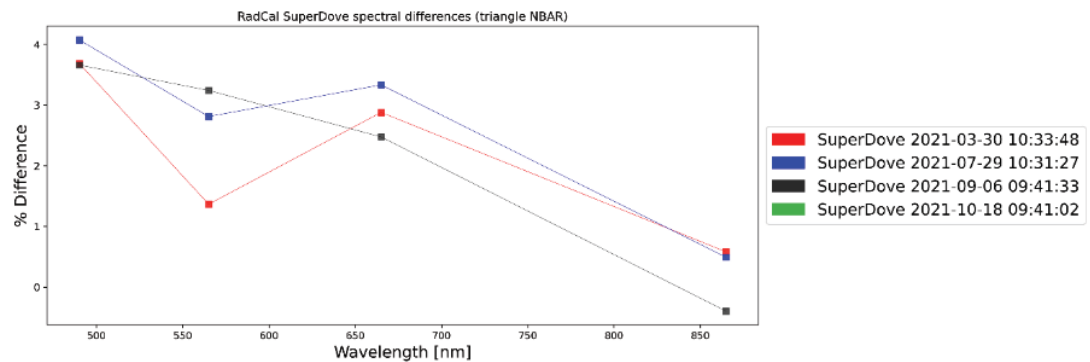


Figure 3-4: Spectral plot of the percentage differences between SuperDove and convolved RadCalNet data for La Crau.

Then, similarly for Gobabeb (GONA), the comparison of the SuperDove data and convolved RadCalNet data is shown in Figure 3-7.

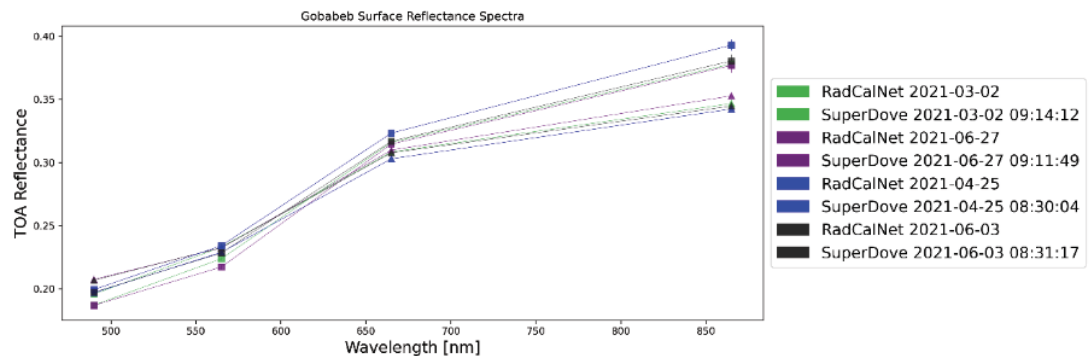


Figure 3-5: Comparison of SuperDove data to RadCalNet convolved to the SuperDove bands for the Gobabeb site.

Figure 3-6 shows the calculated percentage difference between the SuperDove and convolved RadCalNet data for Gobabeb. The Blue and Green bands have higher values than the RadCalNet data for three of the four products but generally the values are lower.

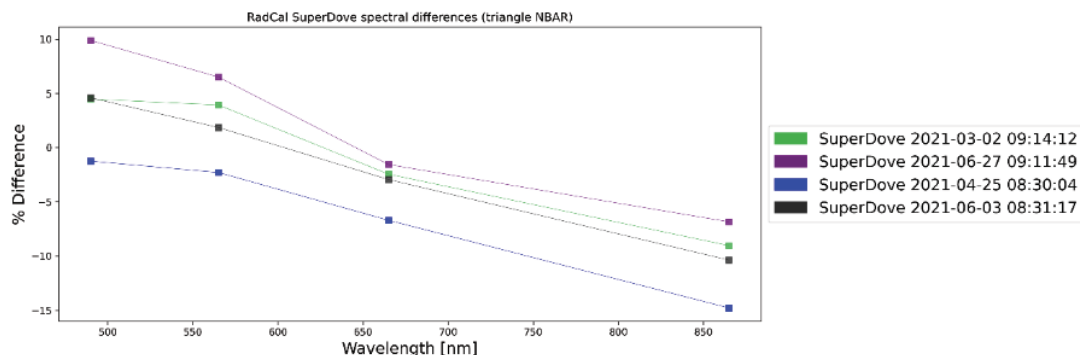


Figure 3-6: Spectral plot of the percentage differences between SuperDove and convolved RadCalNet data at Gobabeb.

3.4 Temporal Radiometric Calibration Accuracy (Stability)

3.4.1 Method - PICS

This method is based on two main processing stages, explained in the figure above:

- Estimate the reference top of atmosphere spectra by using the calibration reference (Sentinel-2 data).
- Use the reference spectra to simulate the reference measurements depending on the sensor to be evaluated.

The first EDAP SuperDove Technical Note [RD-8] shows the details.

3.4.2 Results – PICS

The plan was to undertake a PICS comparison over Libya-4, but the supplied products did not overlap either each other or the defined location for such comparisons; see Figure 3-7. Therefore, as a results of discussions with Planet, time-series products were analysed instead; see Sections 3.4.3 and 3.4.4.



Figure 3-7: Distribution of SuperDove Libya-4 acquisitions versus the centre of the Libya-4 PICS location (small rectangle) and Sentinel-2 scene for scale; scenes overlaid on Bing aerial imagery.

3.4.3 Method – RadCalNet

The methodology was that followed for the absolute radiometric calibration (see Section 3.3), but instead of plotting the spectra, a time-series plot has been generated. Rather than choosing all dates available for the Analysis Ready and Fusion data, the values extracted corresponded to the Level 3 Orthorectified products used for the Absolute Radiometric Calibration analysis.

3.4.4 Results – RadCalNet

Figure 3-8 shows the results of the time-series analysis with data plotted for the supplied four bands and the three datasets: Analysis Ready (square), Fusion (triangle) and RadCalNet (star) extracted at 12:00 (midday) as these products don't have an associate time due to them being composites.

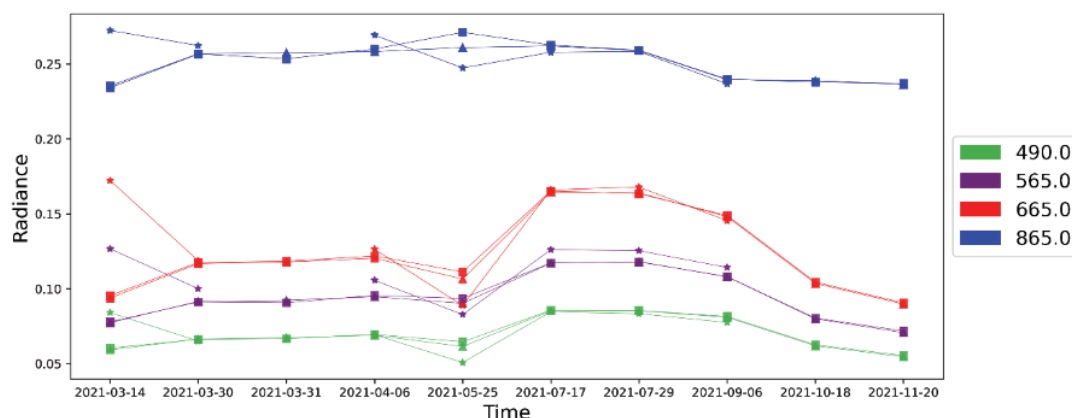


Figure 3-8: Comparison of the Planet Analysis Ready (square), Fusion (triangle) and RadCalNet (star) data over La Crau in terms of the Surface Reflectance for dates throughout 2021 corresponding to the L3 products.

Generally, there is a close agreement between the three datasets, with dates of difference being 14/03/2021 when RadCalNet was higher and 25/05/2021 when there was a divergence between the three datasets. Therefore, in Figure 3-9, a visual comparison of the products for these two dates are shown. In the Analysis Ready products there are missing areas of data, likely due to cloud, which have been filled in the Fusion products. Also, not easily visible in the figure but present just below the missing are in the 14/03/2021 products and, there are some anomalies like to be caused by cloud in the Analysis Ready products that have been removed – red/green fuzzy patches. Interestingly in the 25/05/2021 products, a single field in the top right has become (visually) a lighter shade of green.

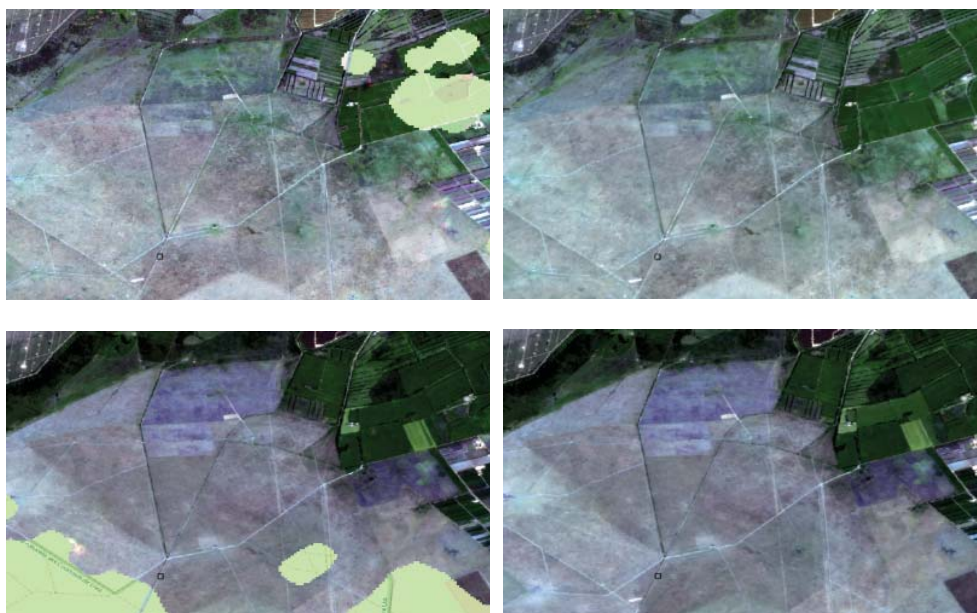


Figure 3-9: Visual comparison of the RGB pseudo-true colour composites for the Planet Analysis Ready (left) and Fusion (right) products for the 14/03/2021 (top) and 25/05/2021 (bottom) overlaid on OpenStreetMap. The small square towards the bottom left is the location of the La Crau RadCalNet site.

3.5 Results Compliance

The absolute radiometric calibration differences from all matchups, Figure 3-4, are shown in Table 3-4 with the average calculated and then colour coded according to whether the average values are larger or smaller than the latest Planet assessment [RD-13]. Also, the results from the previous EDAP Technical Note [RD-8] are included. Only in the Blue band is our estimate of percentage difference with RadCalNet significantly higher for both RadCalNet sites.

Table 3-4: Comparison of the RadCalNet data matchups

| | TOA Reflectance Difference (%) | | | |
|---|--------------------------------|-------------|--------------|---------------|
| | Blue | Green | Red | NIR |
| <i>La Crau / RadCalNet comparison at La Crau from Figure 3-4: 30/03/2021</i> | 3.69 | 1.37 | 2.88 | 0.58 |
| <i>La Crau / RadCalNet comparison at La Crau from Figure 3-4: 29/07/2021</i> | 4.07 | 2.81 | 3.33 | 0.49 |
| <i>RadCalNet comparison at La Crau from Figure 3-4: 06/09/2021</i> | 3.66 | 3.24 | 2.47 | -0.40 |
| Average differences for La Crau | 3.81 | 2.47 | 2.89 | 0.22 |
| <i>RadCalNet comparison at Gobabeb from Figure 3-6: 02/03/2021</i> | 4.47 | 3.93 | -2.46 | -9.04 |
| <i>RadCalNet comparison at Gobabeb from Figure 3-6: 27/06/2021</i> | 9.89 | 6.51 | -1.56 | -6.85 |
| <i>RadCalNet comparison at Gobabeb from Figure 3-6: 25/04/2021</i> | -1.25 | -2.30 | -6.71 | -14.79 |
| <i>RadCalNet comparison at Gobabeb from Figure 3-6: 03/06/2021</i> | 4.59 | 1.85 | -2.95 | -10.37 |
| Average differences for Gobabeb | 4.43 | 2.50 | -3.42 | -10.26 |
| RadCalNet comparison at La Crau from the previous EDAP Technical Note [RD-8] | 2.2 | 0.5 | 1.2 | 1.2 |
| Absolute accuracy compared to RadCalNet from six months of data that equated to 249 crossovers, Q1-2023 [RD-13]* | 1.96 | 4.55 | 5.22 | 10.75 |

*In the Q1-2023 Quality Report, the same differences are also given for the Sentinel-2A, Sentinel-2B and Landsat 8 comparison which is suspicious.

4. DETAILED VALIDATION – GEOMETRIC

4.1 Introduction

The geometric analysis is based on a comparison to a reference (SPOT-5) image that is considered highly characterised. For the work undertaken, described in detail within this Section, the overall approach to the geolocation validation is graded as 'Good'. In terms of the individual elements, absolute geometry and inter-band registration is graded as 'Excellent' while the MTF is graded as 'Basic' because it was considered limited, and the temporal stability is graded as 'Good' because it is a new analysis.

4.2 Data

Data over La Crau were assessed for geolocation accuracy, and are listed in Table 4-1.

Table 4-1. La Crau data used to assess the geometric accuracy.

| Constellation | Dates | Satellites |
|---------------|------------|------------|
| Flock-4V | 30/03/2021 | 2403 |
| | 06/04/2021 | 2403 |
| | 29/07/2021 | 2426 |
| Flock-4S | 06/09/2021 | 2423 |
| | 18/10/2021 | 2423 |
| | 20/11/2021 | 2423 |
| Flock-4EP | 25/05/2021 | 2251 |
| | 09:47:58 | 2251 |
| | 25/05/2021 | 2251 |
| | 09:48:01 | 2251 |
| | 25/10/2021 | 2251 |

4.3 Absolute Geolocation Accuracy

4.3.1 Method

An image2image comparison by using a dense image matching technique, called the Kanade-Lucas-Tomasi (**KLT**) feature tracker, was applied between the reference satellite imagery and Planet acquisitions over La Crau. The KARIOS tool, [RD-6], was used for this purpose. The results were evaluated by statistical measurements, and also visually.

4.3.2 Results

KARIOS was run for each product versus a reference SPOT-5 product (2.5 m accuracy) used for previous EDAP analyses [RD-8]. The results are summarised in Table 4-2 in terms of the statistics for each comparison.

Table 4-2: Absolute geolocation results.

| Site & Data | RMSE X (m) | σ X (m) | RMSE Y (m) | σ Y (m) | RMSE XY (m) | CE90 (m) |
|----------------------------------|------------|----------------|------------|----------------|-------------|----------|
| 29/07/2021 2426 - Flock-4V | 1.68 | 1.65 | 2.20 | 2.18 | 2.77 | 4.00 |

| Site & Data | RMSE X (m) | σ X (m) | RMSE Y (m) | σ Y (m) | RMSE XY (m) | CE90 (m) |
|---|--------------------------------|----------------|------------|----------------|-------------|----------|
| 30/03/2021 2403 - Flock-4V | 3.12 | 3.06 | 4.19 | 2.83 | 5.22 | 7.18 |
| 06/04/2021 2403 - Flock-4V | 1.84 | 1.84 | 2.28 | 2.27 | 2.93 | 3.74 |
| 20/11/2021 2423 - Flock-4S | 5.44 | 3.15 | 2.53 | 2.53 | 6.00 | 7.64 |
| 06/09/2021 2423 - Flock-4S | 3.62 | 3.35 | 2.40 | 2.26 | 4.34 | 6.15 |
| 18/10/2021 2423 - Flock-4S | 3.00 | 2.70 | 2.57 | 2.30 | 3.94 | 5.60 |
| 25/10/2021 2251 - Flock-4EP | 2.34 | 2.26 | 2.43 | 2.19 | 3.37 | 4.61 |
| 25/05/2021 2251 - Flock-4EP 09:47:58 | No overlap with SPOT-5 product | | | | | |
| 25/05/2021 2251 - Flock-4EP | No overlap with SPOT-5 product | | | | | |

4.4 Temporal Geolocation Accuracy

The 4S_Temporal dataset provided by Planet (SD.38, 39, 40, 41, 42) was supposed to contain five separate images over La Crau for temporal geolocation assessment, but the images were not overlapping. Therefore, instead, through direct contact with Planet, access was given to the trial Analysis Ready PlanetScope Backfill dataset.

4.4.1 Method

The method was the same as for the absolute geolocation accuracy (see Section 4.3), but the input dataset was the Analysis Ready PlanetScope Backfill data. One of the two tiles covering the La Crau site, 31N/27E-200N, was chosen, and the reference SPOT-5 product was compared for every available tile for the time-series of data between 01/01/2018 and 23/07/2023 – 1329 tiles in total. The output, mean RMSE in the X and Y direction, from each tile was then used to generate histograms for the whole dataset.

4.4.2 Results

The histograms for the mean RMSE values in the X and Y directions are shown in Figure 4-1 and Figure 4-2, respectively. In the X direction, see Figure 4-1, the RMSE spread is mainly less than 4 m with a peak of around 2 m compared to the reference SPOT-5 product.

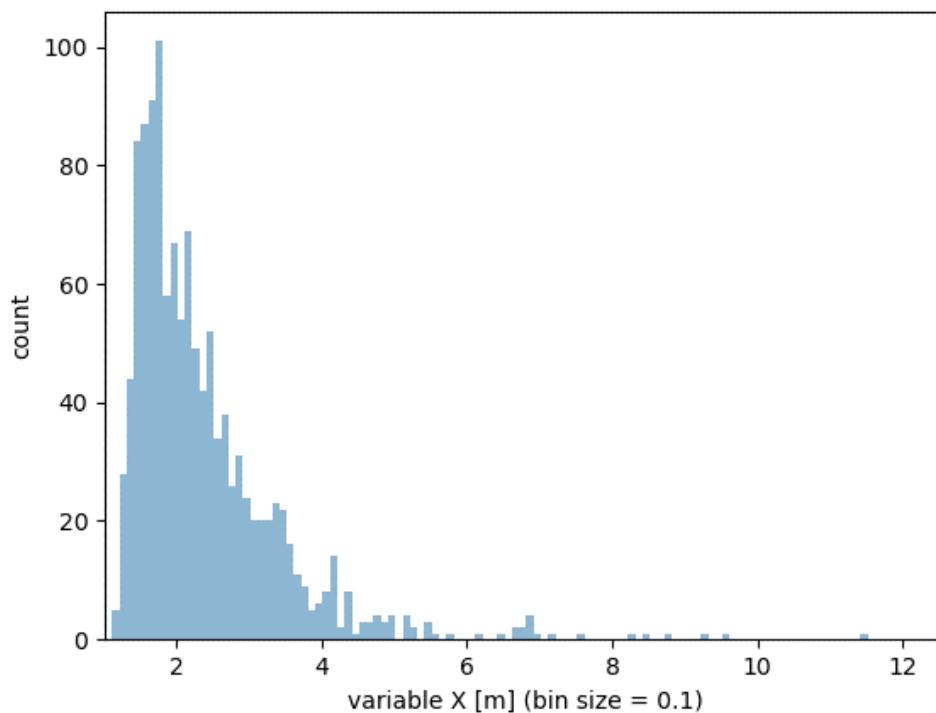


Figure 4-1: Summary histogram of the KARIOS derived RMSE X for the La Crau Analysis Ready PlanetScope Backfill data (tile 31N/27E-200N) obtained between 01 January 2018 and 23 July 2023.

In the Y direction, see Figure 4-2, the RMSE spread is broader, mainly between 2 and 5 m, with a peak around 2.5 m compared to the reference SPOT-5 product.

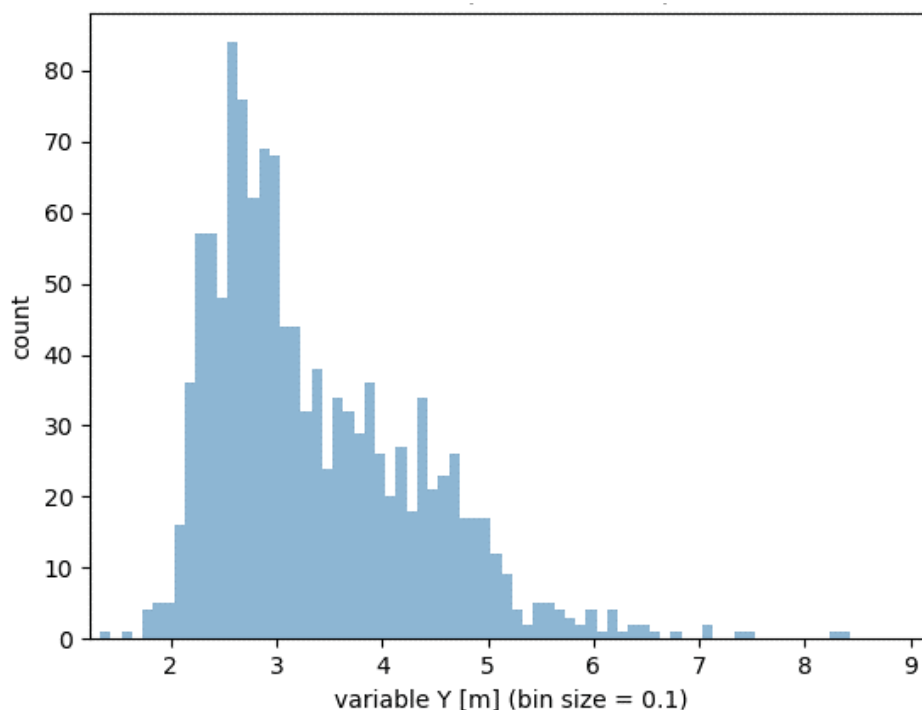
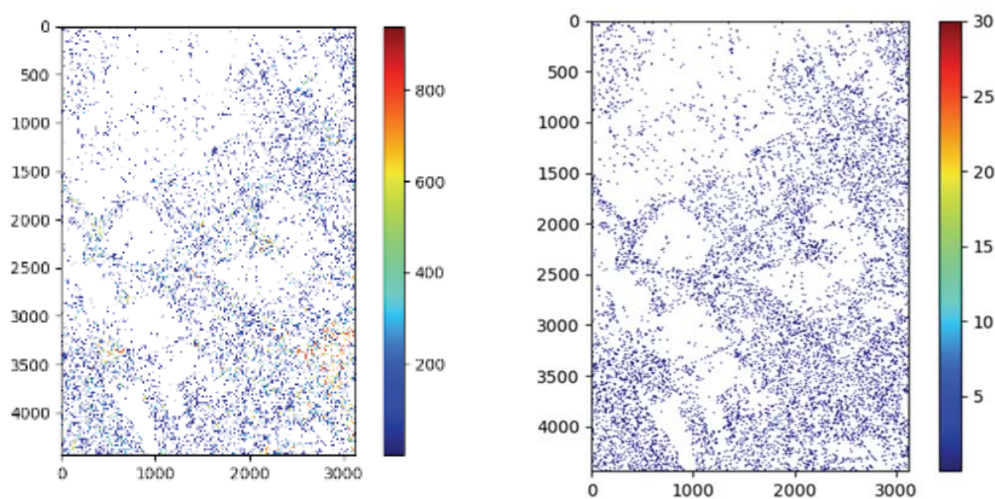


Figure 4-2: Summary histogram of the KARIOS derived RMSE Y for the La Crau Analysis Ready PlanetScope Backfill data (tile 31N/27E-200N) obtained between 01 January 2018 and 23 July 2023.

Spatially, the variations in the temporal RMSE are shown in Figure 4-3. It can be seen that the magnitude is relatively homogeneous while the orientation does vary across the tile.



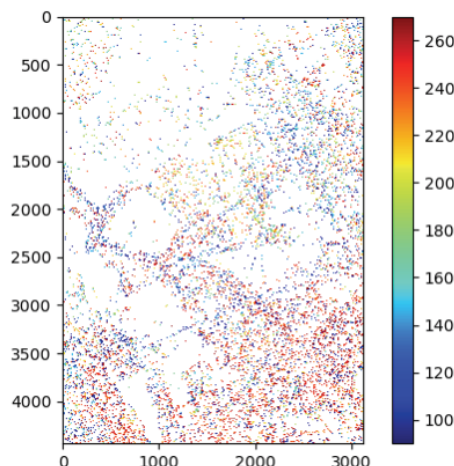


Figure 4-3: Visualisation of temporal RMSE as images: count (top left), temporal average magnitude (top right) and temporal average orientation (bottom).

4.5 Inter-band Registration Accuracy

4.5.1 Methods

The objective is to assess the co-registration between bands. For a given product, several band twins are considered, namely (Green, Blue), (Green, Red), (Green, NIR), and the geometry of the two image grids in the twin, are compared. The grids are compared by using a dense image matching technique: for any pixel location in the image space, a displacement, D , in both line (y) / pixel (x) direction, is computed.

The post-processing of image-matching results is an essential stage before producing accuracy statistics and the related error budget.

4.5.2 Results

The results in Table 4-3 showed that the matching between the Green and other (Blue, Red and NIR) bands generally revealed larger differences for the NIR band.

Table 4-3: Inter-band registration results.

| Site & Data | Band twin | RMSE X (m) | σ X (m) | RMSE Y (m) | σ Y (m) | RMSE XY (m) | CE90 (m) |
|--------------------------------|-----------|------------|----------------|------------|----------------|-------------|----------|
| 29/07/2021 2426 Flock-4V | G-B | 8.06 | 8.03 | 8.54 | 8.51 | 11.75 | 17.92 |
| | G-R | 8.26 | 8.25 | 7.37 | 7.32 | 11.07 | 16.42 |
| | G-NIR | 7.67 | 7.65 | 7.11 | 7.08 | 10.46 | 15.49 |
| 30/03/2021 2403 Flock-4V | G-B | 2.80 | 2.79 | 3.01 | 3.01 | 4.11 | 6.80 |
| | G-R | 2.59 | 2.59 | 2.75 | 2.75 | 3.78 | 6.25 |
| | G-NIR | 5.83 | 5.83 | 6.38 | 6.38 | 8.64 | 14.14 |
| 06/04/2021 | G-B | 1.39 | 1.39 | 1.49 | 1.48 | 2.04 | 3.05 |

| Site & Data | Band twin | RMSE X (m) | σ X (m) | RMSE Y (m) | σ Y (m) | RMSE XY (m) | CE90 (m) |
|---|--------------|---------------|----------------|---------------|----------------|----------------|----------|
| 2403 Flock-4V | G-R | 1.38 | 1.38 | 1.48 | 1.46 | 2.03 | 3.05 |
| | G-NIR | 3.47 | 3.45 | 3.56 | 3.56 | 4.97 | 7.87 |
| 20/11/2021 2423 Flock-4S | G-B | 7.67 | 7.66 | 7.86 | 7.85 | 10.98 | 16.72 |
| | G-R | 8.43 | 8.42 | 8.10 | 8.10 | 11.70 | 17.94 |
| | G-NIR | 8.92 | 8.92 | 8.48 | 8.47 | 12.31 | 18.67 |
| 06/09/2021 2423 Flock-4S | G-B | 2.34 | 2.32 | 2.19 | 2.19 | 3.20 | 5.35 |
| | G-R | 2.18 | 2.18 | 2.06 | 2.06 | 3.00 | 4.95 |
| | G-NIR | 4.45 | 4.44 | 4.52 | 4.52 | 6.34 | 10.70 |
| 18/10/2021 2423 Flock-4S | G-B | 1.51 | 1.51 | 1.45 | 1.45 | 2.10 | 3.05 |
| | G-R | 1.30 | 1.30 | 1.23 | 1.23 | 1.79 | 2.41 |
| | G-NIR | 2.86 | 2.86 | 2.86 | 2.86 | 4.05 | 6.26 |
| 25/10/2021 2251 Flock-4EP | G-B | 1.57 | 1.57 | 1.55 | 1.55 | 2.21 | 3.39 |
| | G-R | 1.41 | 1.41 | 1.34 | 1.34 | 1.94 | 2.58 |
| | G-NIR | 3.03 | 3.03 | 3.29 | 3.28 | 4.47 | 6.64 |
| 25/05/2021 2251 Flock-4EP 09:47:58 | G-B | 0.84 | 0.84 | 0.76 | 0.76 | 1.14 | 1.69 |
| | G-R | 0.82 | 0.81 | 0.75 | 0.74 | 1.11 | 1.62 |
| | G-NIR | 2.44 | 2.43 | 2.48 | 2.48 | 3.48 | 4.99 |
| 25/05/2021 2251 Flock-4EP 09:48:01 | G-B | 0.99 | 0.99 | 0.80 | 0.79 | 1.27 | 1.60 |
| | G-R | 0.93 | 0.92 | 0.76 | 0.75 | 1.20 | 1.59 |
| | G-NIR | 2.26 | 2.25 | 1.98 | 1.97 | 3.01 | 4.47 |

4.6 Results Compliance

As shown in Table 4-2, the measured absolute accuracy is within the product specification accuracy for the PlanetScope L3B (orthorectified) products i.e., of less than 10 m RMSE stated in [RD-7]. In the previous EDAP technical note [RD-8], the RMSE was calculated to be slightly above the stated specification and there was a query as to whether the accuracy in the relative horizontal direction was not as good as in the relative vertical direction. From Figure 4-4, there is no evidence of this difference according to the relative direction as the difference between the two is smaller than the standard deviation.

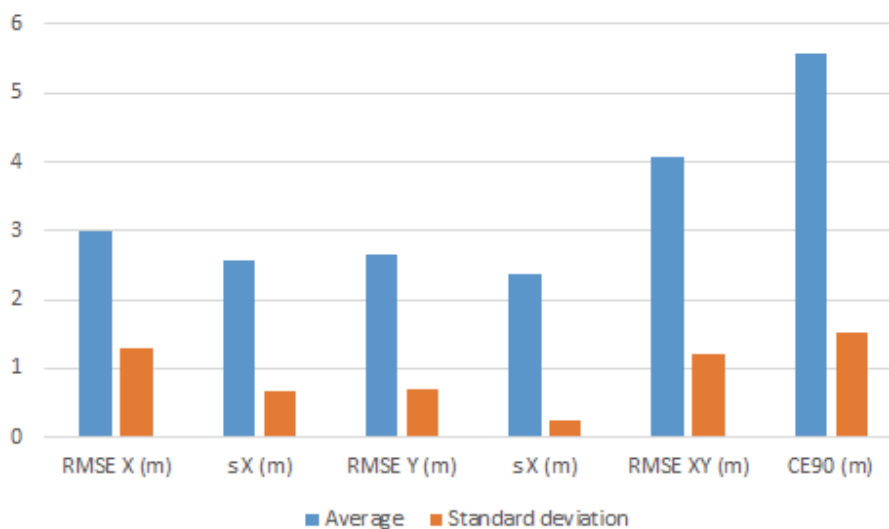


Figure 4-4: Absolute geolocation assessment: plot of all the individual results shown in Table 4-2 as the average and standard deviation.

Figure 4-5 shows coordinate discrepancy plots expressed as angular and radial errors for an example product, 29/07/2021. As shown, the analysis is only performed for matching areas covered by the monitored and reference products.

Errors overview

Monitored : 20210729_103127_02_2426_3B_SkySat.tif
Reference : 20210330_103348_58_2403_3B_SPOT.tif

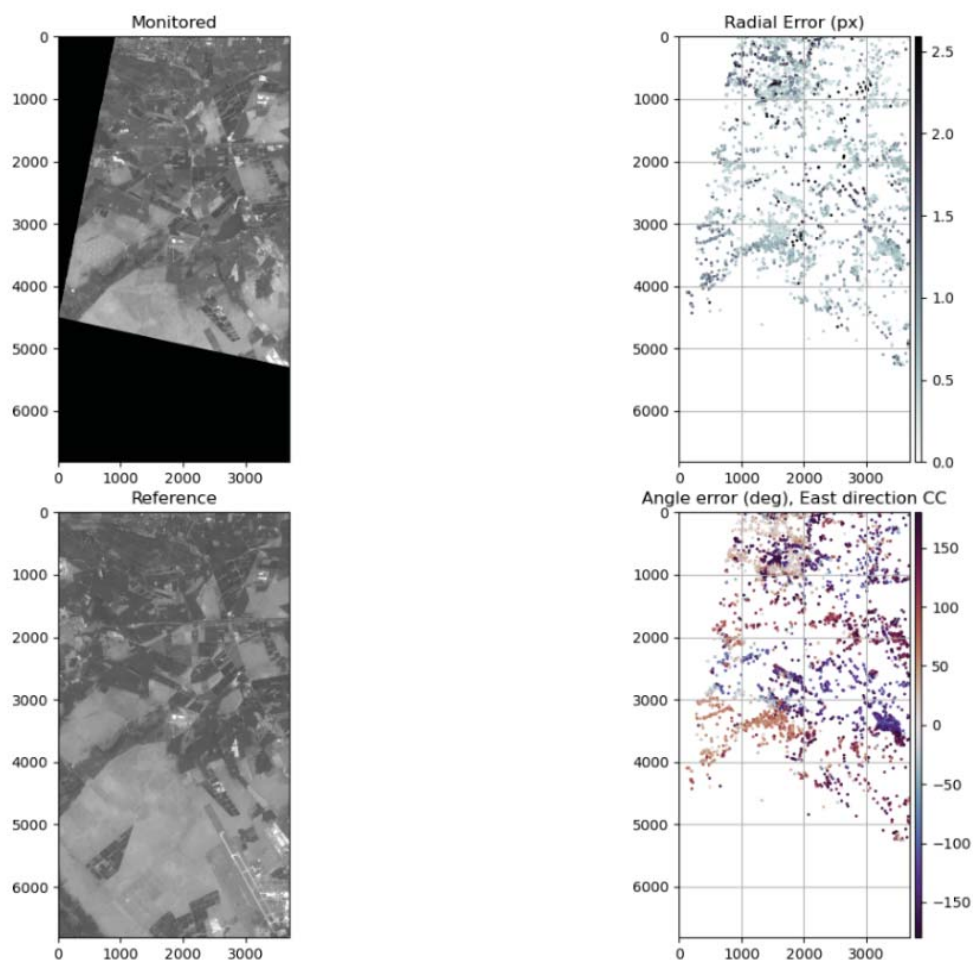


Figure 4-5: Inter-band discrepancy plots (angular and radial errors) for 29/07/2021 over La Crau.

Figure 4-6 shows the statistical results over the La Crau site for different bands when performing the inter-band registration assessment. As in the previous EDAP technical note [RD-8], inter-band registration accuracy using image matching showed good agreement between the Blue, Green and Red bands, with a larger displacement for the NIR band.

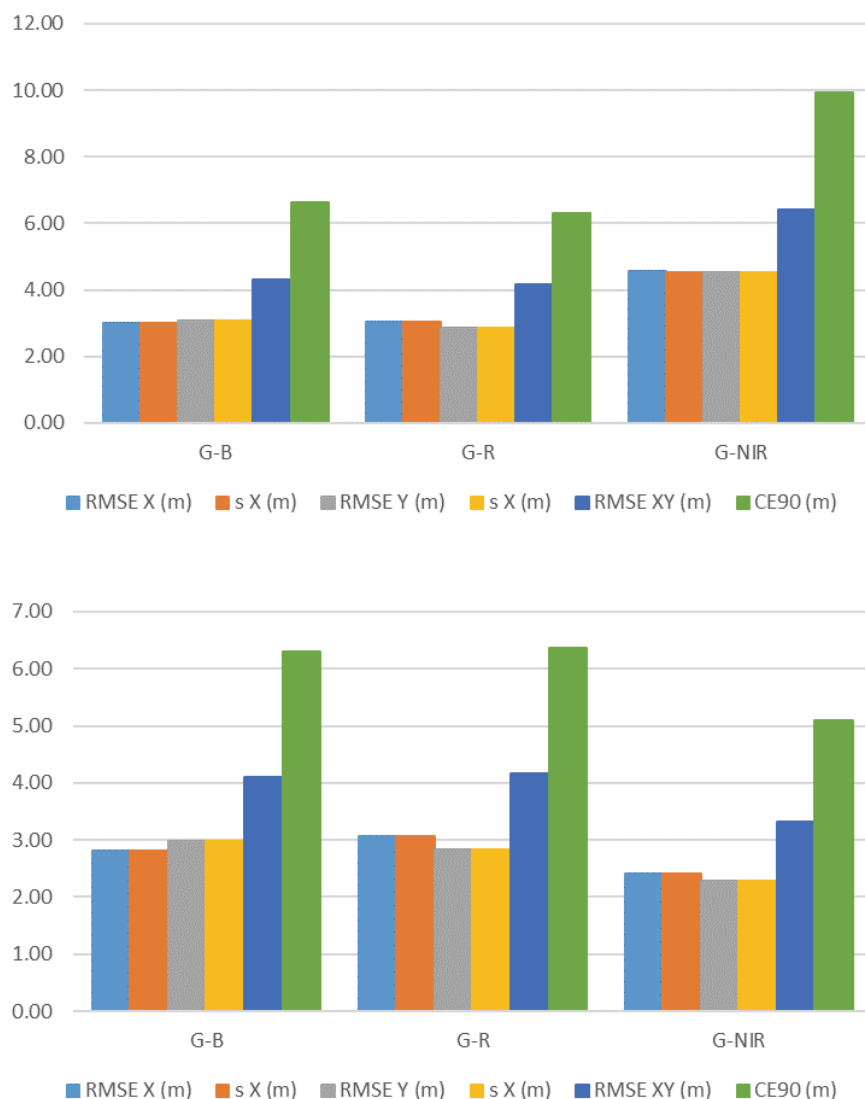


Figure 4-6: Inter-band accuracy assessment: plot of all the results as the average (top) and standard deviation (bottom).

In the previous EDAP technical note [RD-8], the temporal geometric accuracy using image matching between SuperDove products showed some variation between products. The mean errors were sometimes less than one pixel, but not always, the results indicated some inconsistency between satellites. For this technical note, the assessment has been performed using the trial Analysis Ready products. The histograms of all calculated RMSE X and RMSE Y values, shown in Figure 4-1 and Figure 4-2, respectively, have a spread of values that reflects what's seen in the L3 orthorectified products and there is some spread but no indication of significant differences such as a bi-modal distribution.

5. DETAILED VALIDATION – IMAGE QUALITY

The image quality assessments of SuperDove products were performed by using the following distinct approaches:

- Visual Inspection of Image and Data Mask
- Signal-to-Noise Ratio
- Modulation Transfer Function Analysis

Image Interpretability was assessed in the first EDAP SuperDove Technical Note [RD-8], and it was decided this did not need to be reassessed.

5.1 Visual inspections

5.1.1 Method

Each product in the dataset was opened inside QGIS and inspected visually for any obvious defects or interesting artefacts. Edge features (roads, rivers, etc.) were checked for alignment with the underlying geographical map (OpenStreetMap).

First-look inspection used the multispectral image that is displayed in QGIS. Native-resolution display is at a scale of 1:11,339; however, whole-scene inspection took place at a scale of approximately 1:90,000. When anomalies or areas of interest were noticed, further investigation at higher resolution or using separate bands would take place.

5.1.2 Results

5.1.2.1 Usable Data Mask

5.1.2.1.1 Information

Details on the contents of the Usable Data Mask (**UDM2**) are available online at <https://developers.planet.com/docs/data/udm-2/>; some of that information is reproduced below.

The JSON metadata file that comes with each product contains high-level quality information, as shown in Table 5-1.

Table 5-1: Mask information from the JSON metadata

| Field | Type | Value Range | Description |
|--------------------------|------|-------------|--|
| clear_percent | int | [0-100] | Percent of clear values in the dataset. Clear values represent scene content areas (non-blackfilled*) that are deemed to be not impacted by cloud, haze, shadow and/or snow. |
| clear_confidence_percent | int | [0-100] | percentage value: per-pixel algorithmic confidence in 'clear' classification |

| Field | Type | Value Range | Description |
|--|------|-------------|--|
| cloud_percent | int | [0-100] | Percent of cloud values in the dataset. Cloud values represent scene content areas (non-blackfilled) that contain opaque clouds, which prevent reliable interpretation of the land cover content. |
| heavy_haze_percent | int | [0-100] | Percent of heavy haze values in the dataset. Heavy haze values represent scene content areas (non-blackfilled) that contain thin low altitude clouds, higher altitude cirrus clouds, soot, and dust, which allow fair recognition of land cover features, but not having reliable interpretation of the radiometry or surface reflectance. |
| light_haze_percent | int | [0-100] | Percent of light haze values in the dataset. Light haze values represent scene content areas (non-blackfilled) that contain thin low altitude clouds, higher altitude cirrus clouds, soot and dust which allow reliable recognition of land cover features, and have up to +/-10% uncertainty on commonly used indices (EVI and NDWI). |
| shadow_percent | int | [0-100] | Percent of shadow values in the dataset. Shadow values represent scene content areas (non-blackfilled) that are not fully exposed to the solar illumination as a result of atmospheric transmission losses due to cloud, haze, soot and dust, and therefore do not allow for reliable interpretation of the radiometry or surface reflectance. |
| snow_ice_percent | int | [0-100] | Percent of snow and ice values in the dataset. Snow_ice values represent scene content areas (non-blackfilled) that are hidden below snow and/or ice. |
| visible_percent | int | [0-100] | Visible values represent the fraction of the scene content (excluding the portion of the image which contains blackfill) which is comprised of clear, light haze, shadow, snow/ice categories, and is given as a percentage ranging from zero to one hundred. |
| visible_confidence_percent | int | [0-100] | Average of confidence percent for clear_percent, light_haze_percent, shadow_percent and snow_ice_percent |
| *Blackfilled content refers to empty regions of a scene file that have no value. | | | |

A UDM2 multi-band GeoTIFF file is also delivered with the product; the contents of this UDM2 are shown in Table 5-2.

Table 5-2: Contents of multi-band UDM2 GeoTIFF file

| UDM2 band | Description | Pixel Value Range | Interpretation |
|-----------|-----------------|-------------------|--|
| band 1 | Clear map | [0, 1] | 0: not clear, 1: clear |
| band 2 | Snow map | [0, 1] | 0: no snow or ice, 1: snow or ice |
| band 3 | Shadow map | [0, 1] | 0: no shadow, 1: shadow |
| band 4 | Light haze map | [0, 1] | 0: no light haze, 1: light haze |
| band 5 | Heavy haze map | [0, 1] | 0: no heavy haze, 1: heavy haze |
| band 6 | Cloud map | [0, 1] | 0: no cloud, 1: cloud |
| band 7 | Confidence map | [0-100] | percentage value: per-pixel algorithmic confidence in classification |
| band 8 | Unusable pixels | -- | Equivalent to the UDM asset. For the PlanetScope 8th Band, the bits are as follows. Bit 0: Black fill, Bit 1: Likely cloud, Bit 2: Blue (Band 2) is anomalous, Bit 3: Green (Band 4) is anomalous, Bit 4: Red (Band 6) is anomalous, Bit 5: Red Edge (Band 7) is anomalous, Bit 6: NIR (Band 8) is anomalous, Bit 7: Coastal Aerosol (Band 1) and/or Green-I (Band 3) and/or Yellow (Band 5) is anomalous. See Planet's Imagery Specification for complete details. |

The UDM2 classification method is based on machine learning techniques using observation data to train a classification model.

5.1.2.1.2 Assessment

The metadata files of the initial product dataset showed that all had been selected for 0% cloud cover. Therefore, there were no substantial cloudy areas available to assess the masking dataset for cloud. However, some products showed other non-nominal data that could be used in masking assessment, and the multi-band UDM2 GeoTIFF file that accompanies the products did show some pixels categorised as cloudy.

Example 1. Product SD.38: 20211120_094002_84_2423_DOV_MS_L3A. This product showed a fire plume, which was most clearly seen in the MS image (Figure 5-1, left). The relevant UDM2 bands **4** and **5** (light and heavy haze, respectively) showed no flagging for this region or any other, neither did bands **2** and **3** (snow and shadow). The band 7 confidence map (Figure 5-1, right) showed a lowering in classification confidence over this location, but it also showed similar values for urban areas (e.g. top left of images). The level of confidence for the plume area is ~80%.

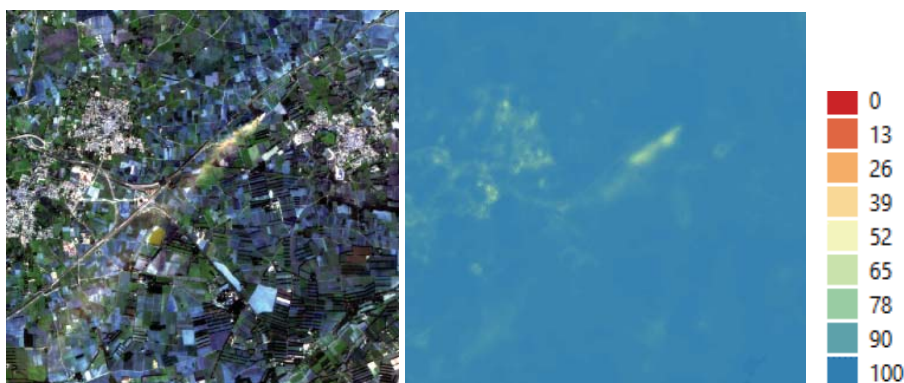


Figure 5-1: Left: Fire plume shown in SD.38 multispectral (plume from top right to lower left); right: UDM2 band 7 confidence map with colour scale.

The areas for which UDM2 band 7 showed the lowest confidence (~50%) are shown in Figure 5-2, which also gives the Band 1 (blue) view from SD.38. It can be seen that the low-confidence areas coincide with high-reflectance areas, which seem to be either industrial-scale greenhouses or solar farms. This is an indication of an area in which the ML training dataset could be improved. Remaining UDM2 bands **1**, **6** and **8** (clear, **cloud** and unusable masks, respectively) also contained flagging in these and other high-reflectance areas, showing that some non-cloudy areas are being flagged as cloudy.

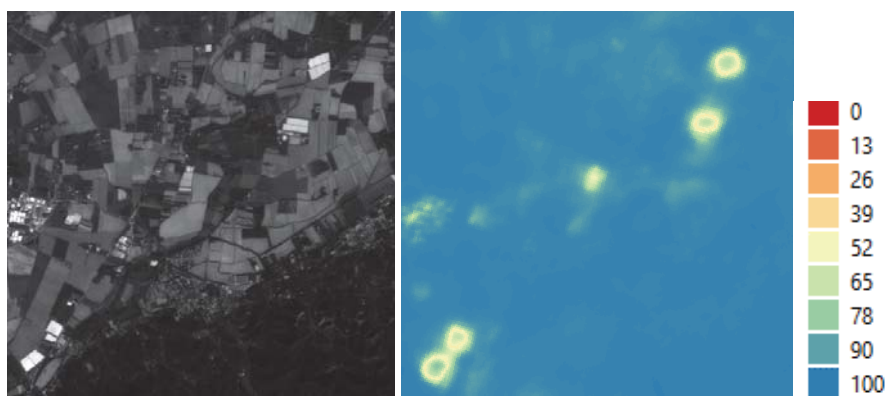


Figure 5-2: Left: SD.38 Band 1 (blue); right: UDM2 band 7 confidence map with colour scale.

5.1.2.2 Other visual inspection findings

Example 2. Product SD.39: 20211018_094058_34_2423_DOV_MS_L3A showed characteristics in the MS image that can be traced to certain features in the spectral bands. Figure 5-3 shows dull and bright orange locations in the multispectral image (left) that appear to be easily recognisable as water bodies in the NIR image (right). The Google© satellite image clearly displays the feature as water bodies, although we concede they are of varying degrees of depth and chalkiness.



Figure 5-3: Left: SD.39 multispectral image; right: NIR band.



Figure 5-4: Google© satellite image close-up of the water bodies shown in Figure 5-3.

5.1.2.3 Metadata information via QGIS

Table 5-3 gives an example of the metadata information from the product when viewed via QGIS.

Table 5-3: Product information as seen by QGIS

| Layer properties | Information |
|-------------------------|---|
| Name | 20211120_094002_84_2423_3B_AnalyticMS |
| Path | C:\Users\...\20211120_094002_84_2423_DOV_MS_L3A\analytic_udm2\20211120_094002_84_2423_3B_AnalyticMS.tif |
| CRS | EPSG:32631 - WGS 84 / UTM zone 31N - Projected |
| Extent | 607245.0000000000000000,4831332.0000000000000000 : 647571.0000000000000000,4860204.0000000000000000 |
| Unit | meters |
| Width | 13442 |
| Height | 9624 |
| Data type | UInt16 - Sixteen bit unsigned integer |
| GDAL Driver Description | GTiff |
| GDAL Driver Metadata | GeoTIFF |
| Dataset Description | C:/Users/.../20211120_094002_84_2423_DOV_MS_L3A/analytic_udm2/20211120_094002_84_2423_3B_AnalyticMS.tif |
| Compression | LZW |

| Layer properties | Information |
|------------------|--------------------------------------|
| Band 1 | STATISTICS_APPROXIMATE=YES |
| | STATISTICS_MAXIMUM=7270 |
| | STATISTICS_MEAN=3105.2983061179 |
| | STATISTICS_MINIMUM=2322 |
| | STATISTICS_STDDEV=344.81595983234 |
| | STATISTICS_VALID_PERCENT=70.13 |
| Band 2 | |
| Band 3 | |
| Band 4 | |
| More information | AREA_OR_POINT=Area |
| | TIFFTAG_DATETIME=2021:11:20 09:40:02 |
| | X : 4481 |
| | Y : 3208 |
| | X : 1494 |
| | Y : 1070 |
| | X : 498 |
| | Y : 357 |
| Dimensions | X: 13442 Y: 9624 Bands: 4 |
| Origin | 607245,4.8602e+06 |
| Pixel Size | 3,-3 |
| Band count | 4 |
| 1 | Band 1: blue |
| 2 | Band 2: green |
| 3 | Band 3: red |
| 4 | Band 4: nir |

5.2 Signal-To-Noise Ratio (SNR)

The SNR is an important image quality indicator. Visual interpretation of an image does not require high SNR data: even in the presence of noise, an operator can identify objects. However, multispectral image processing requires high SNR values to control the measurement's uncertainties as much as possible.

For each band, the SNR value and its corresponding average reference radiance $W \cdot sr^{-1} m^{-2}$ are given. The proposed method herein has already been implemented in the context of other EDAP assessments. A description of the method is provided below.

5.2.1 Method

The SNR is a measure of the mean signal to noise ratio. In the scientific community, two types of SNR are typically measured; the temporal SNR and the spatial SNR. The basic formulation of the SNR is given by:

$$SNR = \frac{\mu}{\sigma}$$

Where:

- μ is the mean signal,
- σ is the standard deviation of the signal.

The herein proposed method estimates the spatial SNR considering the statistical distribution over a set of “small windows” (5 pixels by 5 pixels), whereby referring to the previous mathematical relationship:

- The “mean signal” is defined as the spatial average of a group of pixels in the “small window”;
- Noise is typically defined as the standard deviation of a region of pixels in the “small window”.

Each spectral band image (radiance measurement) is processed with the modified algorithm initially proposed in [RD-19]. The algorithm has been modified to allow the selection of small windows of uniform image intensity (condition 1), and the selection of small windows mostly located over regions with a flat terrain relief (condition 2).

For conducting this SNR assessment, a uniform / bright scene is selected. However, high frequency spatial features may still exist in the image, specifically at locations of sharp transitions (e.g., desert dune summit for Libya-4). To overcome this, image processing is applied to detect high frequency content and filter small windows (image window processing with Sobel operator).

In summary, the different steps within the EDAP SNR algorithm are:

- Create SNR image, considering as input, image converted to radiance measurements, and iterating on “small windows” to compute SNR,
- Compute local statistics over 5 pixels x 5 pixels sliding window on the terrain relief data and the image edge response (Sobel Operator),
- Select the set of “small windows” displaying uniform content and located in flat areas,
- Compute the statistical distribution (histogram) of “small windows” $\frac{\mu}{\sigma}$,
- Location of the peak in the histogram of SNR image is a measure of the system SNR,
- Report the SNR value at the peak and the corresponding mean radiance value.

The SNR is a function of the mean radiance of the landscape. The SNR is usually lower for low value of radiance (dark landscape) because the relative influence of the noise is larger. For large radiances, the SNR increases as the relative influence of the noise decreases.

Further details on the approach can be found in the EDAP Technical Note on Methods and Reference Data for Optical Data Quality Assessments [RD-20].

5.2.2 Results

Due to the method, results might be dependent on the selected Region of Interest (**ROI**). Therefore, ROIs have been selected within both the Libya-4 and La Crau sites, which have been chosen to be relatively limited in features; see **Figure 5-5** and **Figure 5-6**, respectively.

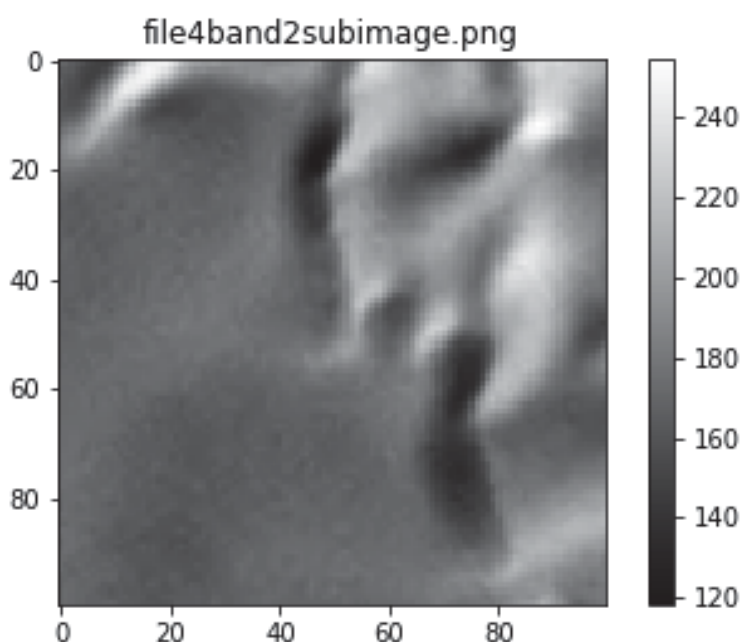
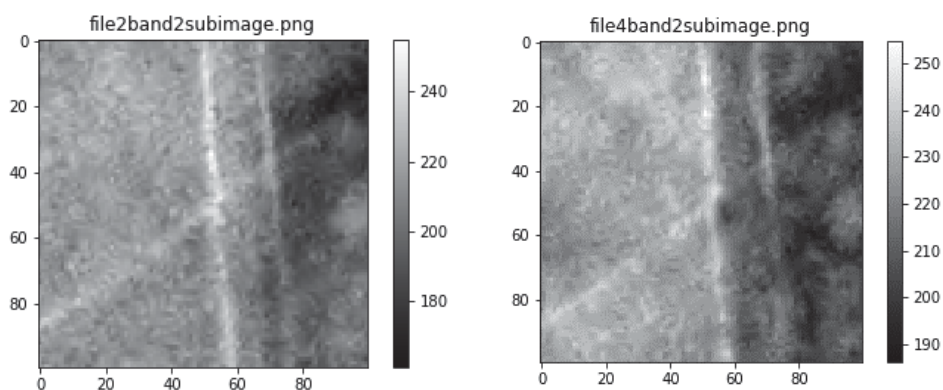


Figure 5-5: Selected area for the Libya-4 SNR analysis: 23/01/2021 2251



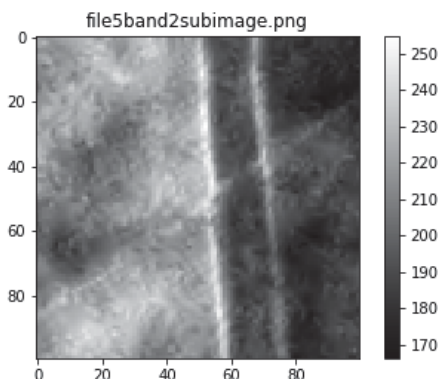


Figure 5-6: Selected area for the La Crau SNR analysis, with three files processed: 30/03/2021 2403, 06/09/2021 2423 and 18/10/2021 2423.

The SNR results for Libya-4 and La Crau are plotted alongside a reference radiance in Figure 5-7 and Figure 5-8, respectively. For Libya-4, the Red band SNR results are better than the SNR results of the other band sand the NIR band is significantly lower than the other bands. For all three products for La Crau, the Red and NIR bands are significantly lower than the other bands.

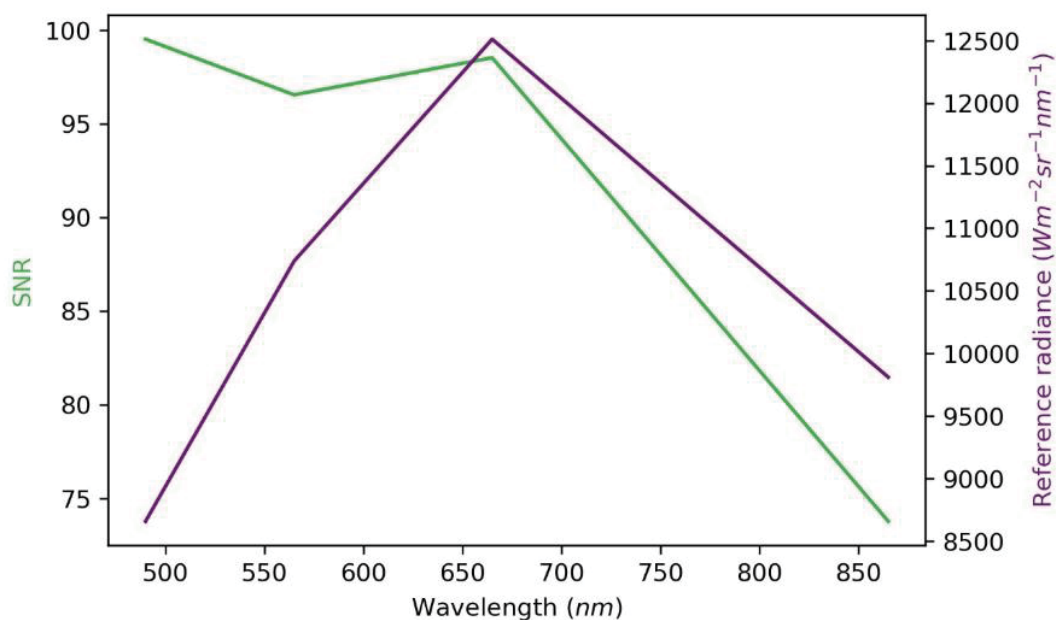


Figure 5-7: Plot of SNR and reference radiance for the Libya-4 product: 23/01/2021 2251

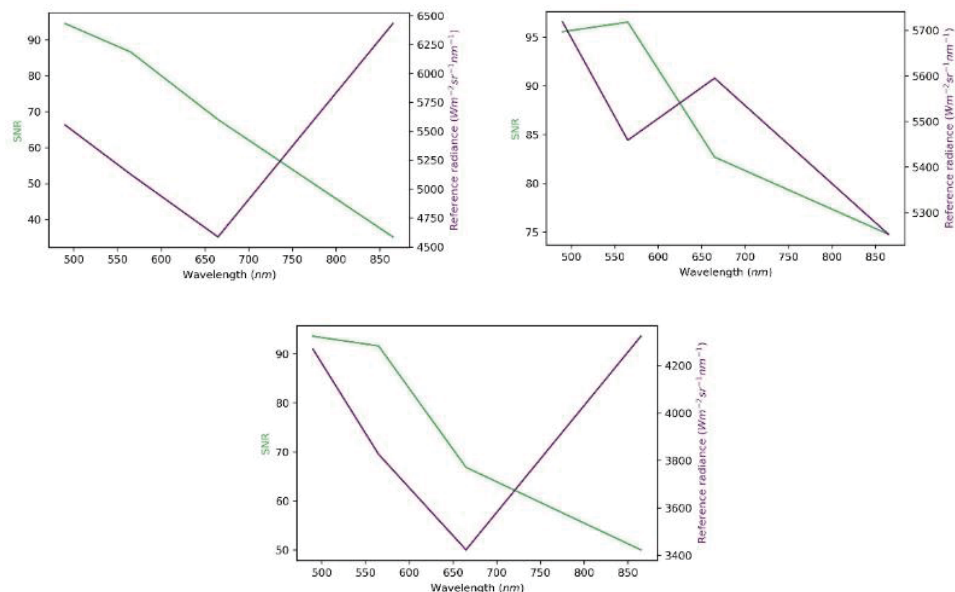


Figure 5-8: Plot of SNR and reference radiance for the La Crau product, with three files processed: 30/03/2021 2403, 06/09/2021 2423 and 18/10/2021 2423.

5.3 Modulation Transfer Function (MTF)

As a measure of the geospatial quality of imagery, the Modulation Transfer Function (**MTF**) of the sensor is often used along with the SNR. It is often used as a measure of image sharpness but has to be checked for each orbit in order to be sure that launch vibrations, transition from air to vacuum, or thermal state have not degraded the sharpness of the images [RD-5].

5.3.1 Data

Data over Baotou assessed for geolocation accuracy are listed in Table 5-4, respectively.

Table 5-4. Baotou data used to assess the data sharpness.

| Constellation | Dates | Satellites |
|---------------|------------|------------|
| Flock-4V | 21/09/2021 | 2426 |
| Flock-4S | 27/03/2021 | 2423 |
| Flock-4EP | 22/03/2021 | 2251 |

5.3.2 Method

Artificial Modulation Transfer Function targets, such as the one in Baotou (China) see **Figure 5-9** is too small to give a fair assessment of imagery from satellites with the GSD of SuperDove. Therefore, we have chosen to conduct a sharpness analysis using the

structure above the MTF target that provide a linear target with a bright/dark contrast (pink box).



Figure 5-9: Baotou MTF target captured on 21/09/2021 shown using the 5 m resolution 4V SuperDove imagery; the pink box is the sub-area chosen for the MTF assessment.

Unlike the products for the other sites, these are L1B to avoid effects due to higher level processing. In attempting to subset all three GeoTIFFs, to support the MTF calculation, issues were encountered with the geometry. If we take the product shown in **Figure 5-9**, running listgeo (using GDAL 3.6.4, released 2023/04/17) resulted in the following was reported:

```
TIFFReadDirectory: Warning, Unknown field with tag 42112 (0xa480)
encountered.
TIFFReadDirectory: Warning, Unknown field with tag 42113 (0xa481)
encountered.
TIFFReadDirectory: Warning, Unknown field with tag 50844 (0xc69c)
encountered.
Geotiff_Information:
  Version: 1
  Key_Revision: 1.0
  Tagged_Information:
    End_Of_Tags.
  Keyed_Information:
    End_Of_Keys.
  End_Of_Geotiff.
```

In addition, when subsetting was attempted with SNAP (9.0.0) it failed as the GeoTIFF information could not be interpreted incorrectly and the subset area was outside the scene;

see **Figure 5-10**. This GeoTIFF information also caused problems when trying to zoom in and the zoomed area jumped from that chosen.

Therefore, the geometry was adjusted via GDAL using the information in the metadata XML file, i.e.

```
gdal_translate 20210322_025200_30_2251_1B_AnalyticMS.tif
20210322_025200_30_2251_1B_AnalyticMS_crs.tif -a_srs EPSG:4326 -
a_ullr 109.3870022863 40.9879403582 109.8389929204 40.7391328559
```

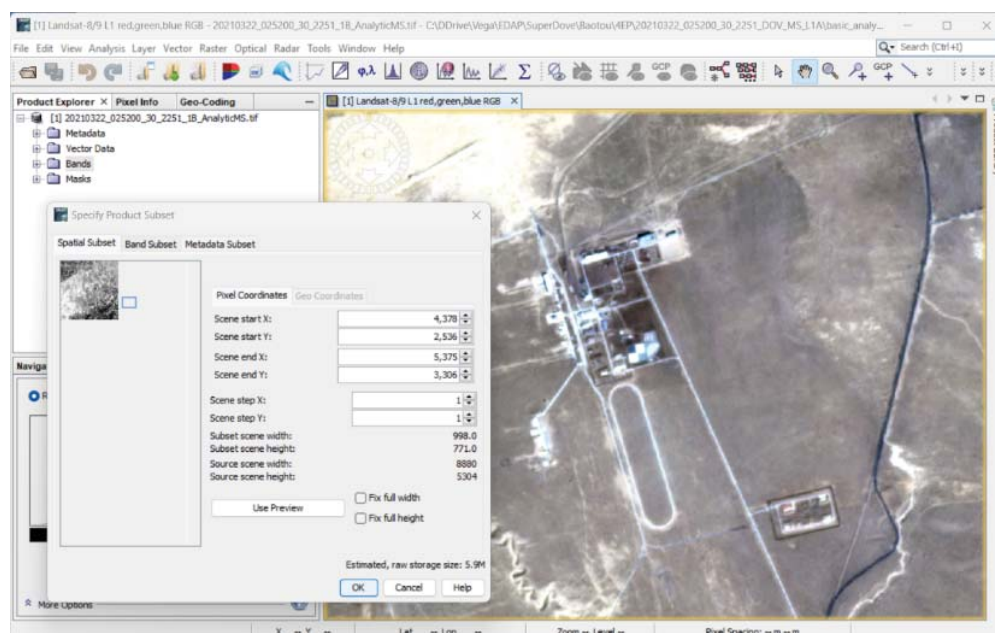


Figure 5-10: Attempt to subset the 4V Baotou product captured on 21/09/2021.

This addition of geometry information using this approach allowed the MTF assessment to be performed using the MTF Estimator QGIS Plugin [RD-21] but was insufficient for the geometry to be accurate. Also, the MTF tool requires vertical rather than horizontal edges. Therefore, the scene was rotated by -90 degrees and then the box for the MTF assessment was manually drawn. The edge is not ideally aligned as it should be a maximum of 5-8 degrees off vertical/horizontal, but rotating by a value other than 90 degrees caused resampling issues that will have impacted the MTF assessment.

5.3.3 Results

Running the MTF analysis for each product, as shown in **Figure 5-11**, results in varying outputs. Also, for there isn't sufficient contrast for all bands and the off vertical/horizontal alignment is not optimal for .

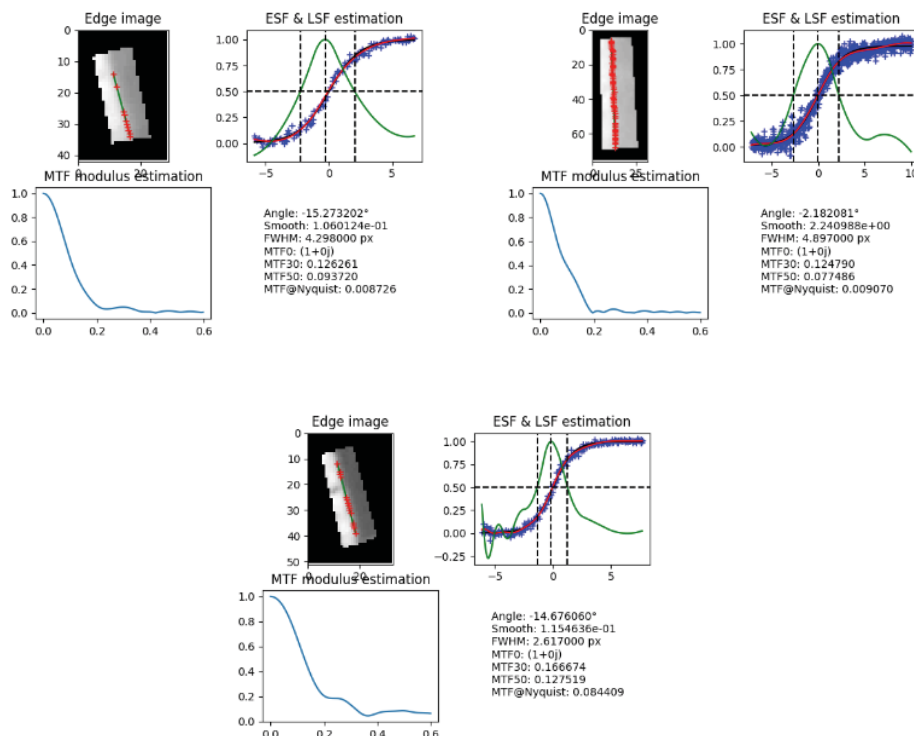


Figure 5-11: Green band MTF outputs for the (top left, top right then bottom middle) 4EP, 4S and 4V Baotou products captured on 22 March, 37 March and 21 September 2021.

5.4 Results Compliance

For SNR, Table 5-5 shows the calculated values at Libya-4 and La Crau alongside the in-flight data extracted by Planet [RD-13]. The values for the Blue and Green bands are higher when calculated by EDAP, but similar, while there are larger differences for the Red and NIR bands but again EDAP's calculated values are higher than that modelled by Planet.

Table 5-5: Average SNR for the Libya-4 and La Crau products

| Scene | SNR | | | |
|-------------------------------|--------|--------|--------|--------|
| | Blue | Green | Red | NIR |
| Libya-4 average | 99.51 | 96.54 | 98.52 | 73.77 |
| La Crau average | 94.56 | 91.59 | 72.45 | 53.31 |
| Modelled SNR, Q1 2023 [RD-13] | 91.035 | 80.514 | 65.167 | 37.304 |

In terms of MTF, Table 5-6 shows the MTF at the Nyquist frequency for all three products but just the Blue and Green bands as the Red and NIR suffered from poor contrast. These results aren't considered sufficient for a suitable conclusion to be drawn but highlight a possible approach for MTF assessment using contrast features occurring within the imagery.

Table 5-6: MTF at the Nyquist frequency for the Baotou products

| Scene | MTF @ Nyquist frequency | |
|-------|-------------------------|----------|
| | Blue | Green |
| 4EP | 0.013728 | 0.008726 |
| 4S | 0.009784 | 0.009070 |
| 4V | 0.067191 | 0.084409 |

APPENDIX A Products analysed from the Mission Test Dataset

| ID | Site | Product | Assessment |
|-------|-------------------|------------------------------------|---|
| SD.1 | La Crau | 20210729_103127_02_2426_DOV_MS_L3A | Absolute radiometry, Absolute geolocation, Inter-band registration |
| SD.2 | La Crau | 20210330_103348_58_2403_DOV_MS_L3A | Absolute radiometry, Absolute geolocation, Inter-band registration, SNR |
| SD.3 | La Crau | 20210406_103352_05_2403_DOV_MS_L3A | Absolute geolocation, Inter-band registration |
| SD.4 | Libya | 20210103_090951_61_2403_DOV_MS_L3A | |
| SD.5 | Libya | 20210403_090922_22_2426_DOV_MS_L3A | |
| SD.6 | Libya | 20210101_091143_95_2426_DOV_MS_L3A | |
| SD.7 | Salon-de-Provence | 20210729_103127_02_2426_DOV_MS_L3A | |
| SD.8 | Salon-de-Provence | 20210108_103714_66_2426_DOV_MS_L3A | |
| SD.9 | Salon-de-Provence | 20210108_103716_92_2426_DOV_MS_L3A | |
| SD.10 | Baotou | 20210921_032935_74_2426_DOV_MS_L1A | MTF |
| SD.11 | Gobabeb | 20210627_091149_38_2426_DOV_MS_L3A | Absolute radiometry |
| SD.12 | Gobabeb | 20210302_091412_16_2426_DOV_MS_L3A | Absolute radiometry |
| SD.13 | Gobabeb | 20211215_090523_03_2426_DOV_MS_L3A | |
| SD.14 | La Crau | 20211120_094002_84_2423_DOV_MS_L3A | Absolute geolocation, Inter-band registration |
| SD.15 | La Crau | 20210906_094133_45_2423_DOV_MS_L3A | Absolute radiometry, Absolute geolocation, Inter-band registration, SNR |
| SD.16 | La Crau | 20211018_094102_94_2423_DOV_MS_L3A | Absolute radiometry, Absolute geolocation, Inter-band registration, SNR |
| SD.17 | Libya | 20211220_081435_74_2449_DOV_MS_L3A | |
| SD.18 | Libya | 20211220_081431_14_2449_DOV_MS_L3A | |
| SD.19 | Salon-de-Provence | 20211120_094002_84_2423_DOV_MS_L3A | |
| SD.20 | Salon-de-Provence | 20211018_094100_64_2423_DOV_MS_L3A | |
| SD.21 | Salon-de-Provence | 20210720_093926_36_245a_DOV_MS_L3A | |
| SD.22 | Salon-de-Provence | 20210711_094111_30_245a_DOV_MS_L3A | |
| SD.23 | Salon-de-Provence | 20210614_094432_78_245a_DOV_MS_L3A | |

| ID | Site | Product | Assessment |
|-------|-------------------|------------------------------------|---|
| SD.24 | Baotou | 20210327_024224_43_2423_DOV_MS_L1A | MTF |
| SD.25 | La Crau | 20211025_095224_69_2251_DOV_MS_L3A | Absolute geolocation, Inter-band registration |
| SD.26 | La Crau | 20210525_094801_08_2251_DOV_MS_L3A | Inter-band registration |
| SD.27 | La Crau | 20210525_094758_79_2251_DOV_MS_L3A | Inter-band registration |
| SD.28 | Libya | 20210129_082802_73_2251_DOV_MS_L3A | |
| SD.29 | Libya | 20210313_082550_05_2251_DOV_MS_L3A | |
| SD.30 | Libya | 20210123_082548_80_2251_DOV_MS_L3A | SNR |
| SD.31 | Salon-de-Provence | 20210827_095228_75_2264_DOV_MS_L3A | |
| SD.32 | Salon-de-Provence | 20210609_095055_76_2264_DOV_MS_L3A | |
| SD.33 | Salon-de-Provence | 20211025_095222_40_2251_DOV_MS_L3A | |
| SD.34 | Baotou | 20210322_025200_30_2251_DOV_MS_L1A | MTF |
| SD.35 | Gobabeb | 20210603_083117_57_2264_DOV_MS_L3A | Absolute radiometry |
| SD.36 | Gobabeb | 20210603_083119_86_2264_DOV_MS_L3A | |
| SD.37 | Gobabeb | 20210425_083004_45_2251_DOV_MS_L3A | Absolute radiometry |
| SD.38 | La Crau | 20211120_094002_84_2423_DOV_MS_L3A | Visual inspection, Mask assessment |
| SD.39 | La Crau | 20211018_094058_34_2423_DOV_MS_L3A | Visual inspection |
| SD.40 | La Crau | 20210906_094135_75_2423_DOV_MS_L3A | |
| SD.41 | La Crau | 20210717_093710_49_2423_DOV_MS_L3A | |
| SD.42 | La Crau | 20210314_094331_43_2423_DOV_MS_L3A | |



[END OF DOCUMENT]